THE JOURNAL OF BIOLOGICAL CHEMISTRY VOL. 287, NO. 2, pp. 1306–1321, January 6, 2012

Plasmodium falciparum Inhibitor-3 Homolog Increases Protein Phosphatase Type 1 Activity and Is Essential for Parasitic Survival*[S]

Received for publication, June 28, 2011, and in revised form, November 18, 2011 Published, JBC Papers in Press, November 28, 2011, DOI 10.1074/jbc.M111.276865

Aline Fréville[‡], Isabelle Landrieu[§1,2], M. Adelaida García-Gimeno[¶], Jérôme Vicogne[‖], Muriel Montbarbon[‡], Benjamin Bertin[‡], Alexis Verger[**], Hadidjatou Kalamou[‡], Pascual Sanz[¶], Elisabeth Werkmeister[‖], Christine Pierrot[‡], and Jamal Khalife[‡1,2,3]

From the [‡]Center for Infection and Immunity of Lille, Inserm U1019-CNRS UMR 8204, University of Lille Nord de France, Institut Pasteur de Lille, 1 Rue du Professeur Calmette, 59019 Lille Cedex, France, the [§]Structural and Functional Glycobiology Unit, UMR8576 CNRS-University of Sciences and Technologies of Lille, 59655 Villeneuve d'Ascq, France, the [¶]Instituto de Biomedicina de Valencia (CSIC) and Centro de Investigación Biomédica en Red de Enfermedades Raras, Jaime Roig, 11, 46010 Valencia, Spain, the [**]IRI-Institut de Recherche Interdisciplinaire USR3078 CNRS-Université Lille1-Université Lille 2, 59658 Villeneuve d'Ascq, France, and the [‖]Institut de Biologie de Lille, UMR8161, BICeL-IFR142, Institut Pasteur de Lille, 1 Rue du Professeur Calmette, 59019 Lille Cedex, France

Background: Little is known about the regulators of phosphatase 1 enzyme activity in *Plasmodium falciparum*.
Results: An activator, its binding motifs, and its nuclear location are presented. Reverse genetics show its essentiality for parasite survival.
Conclusion: There is a potential link between this activator and the nuclear activity of this enzyme.
Significance: This regulator is essential and can be considered as a potential drug target.

Growing evidence indicates that the protein regulators governing protein phosphatase 1 (PP1) activity have crucial functions because their deletion drastically affects cell growth and division. PP1 has been found to be essential in *Plasmodium falciparum*, but little is known about its regulators. In this study, we have identified a homolog of Inhibitor-3 of PP1, named PfI3. NMR analysis shows that PfI3 belongs to the disordered protein family. High affinity interaction of PfI3 and PfPP1 is demonstrated *in vitro* using several methods, with an apparent dissociation constant K_D of 100 nM. We further show that the conserved ^{41}KVVRW^{45} motif is crucial for this interaction as the replacement of the Trp^{45} by an Ala^{45} severely decreases the binding to PfPP1. Surprisingly, PfI3 was unable to rescue a yeast strain deficient in I3 (Ypi1). This lack of functional orthology was supported as functional assays *in vitro* have revealed that PfI3, unlike yeast I3 and human I3, increases PfPP1 activity. Reverse genetic approaches suggest an essential role of PfI3 in the growth and/or survival of blood stage parasites because attempts to obtain knockout parasites were unsuccessful, although the locus of *PfI3* is accessible. The main localization of a GFP-tagged PfI3 in the nucleus of all blood stage parasites is compatible with a regulatory role of PfI3 on the activity of nuclear PfPP1.

Protein phosphatases are well known to play key roles in many biological functions by controlling essential nodes involved in cellular growth, differentiation, and division. The elucidation of many events directed by these enzymes came initially from the discovery of diverse natural toxins that have been found to be potent and specific inhibitors of phosphatases (1–4). It is estimated that ~30% of cellular proteins are phosphorylated by kinases at a given time, implying that they are potentially submitted to a dephosphorylation process by phosphatases to control their activities. Protein phosphatase type 1 (PP1)[4] is considered as one of the major phosphatases involved in the control of numerous dephosphorylation steps. In this context, it has been reported that a decrease of PP1 activity by a reduction of its expression using antisense oligonucleotides resulted in a failure of cell division in a late stage of cytokinesis (5). Conversely, a hyperphosphorylation state of cellular proteins induced by an overexpression of some kinases blocked cell division (6–8), indicating a fundamental role of the phosphorylation/dephosphorylation balance. Taken together, these observations point out that cell vitality and viability must be coordinated through multiple and tight regulations of both kinases and phosphatases. In eukaryotic cells, a large number of endogenous proteins regulating PP1 have been identified, most of which have been found as "permanent" ligands for this enzyme allowing the control of its localization, activity, and/or its specificity (9). These regulators mainly include proteins with a degenerate sequence motif $((K/R)X_{0-1}(V/I)p(F/W)$, known as the RV*X*F-binding motif to PP1 (9). Biochemical, interaction, and genetic studies clearly indicated that PP1 regulators are as crucial as PP1 itself in the control of cell vitality and survival (10). Hence, the multiple functions of PP1 seem to be organized

* This work was supported in part by Inserm, Institut Pasteur de Lille, Université Lille Nord de France, and TGE RMN THC Grant FR-3050, France.
[S] This article contains supplemental Figs. S1–S3 and Tables S1 and S2.
[1] Both authors contributed equally to this work
[2] Member of the CNRS.
[3] To whom correspondence should be addressed. Tel.: 33-320877968; E-mail: jamal.khalife@pasteur-lille.fr.

[4] The abbreviations used are: PP1, protein phosphatase type 1; Ni-NTA, nickel-nitrilotriacetic acid; pNPP, *p*-nitrophenyl phosphate; RU, resonance unit; SPR, surface plasmon resonance.

and to operate according to the binding of distinct regulators. So far, more than 100 regulatory subunits of PP1 have been characterized, leading to a high number of holoenzymes that can explain the multiple and specific functions of this enzyme at different locations (11).

In *Plasmodium falciparum* (Pf), an apicomplexan parasite responsible for most of the morbidity and mortality attributable to human malaria, phosphatase activities and corresponding genes have been identified, including PP1 and PP2A (12–17). The use of natural toxins to phosphatases, such as okadaic acid, indicated that blood stage parasites exhibited a high level of phosphatase activity associated with PP1 (14). In addition, okadaic acid has been shown to inhibit parasite growth *in vitro*, mainly by blocking PP1-like activity (18). In this parasite, very little is known about the role of endogenous regulatory subunits of PP1, although we recently reported the first data on an inhibitory subunit of PfPP1, PfLRR1 (19). The gene product of *PfLRR1* belongs to the leucine-rich repeat protein family and is the ortholog of Sds22 described in yeast (20). We showed that PfLRR1 was able to interact physically with PfPP1 and to down-regulate its phosphatase activity. Our inability to obtain knock-out parasites for *PfLRR1*[5] and the fact that an overexpression of its ortholog in *Toxoplasma gondii* (21) can impair parasite growth suggested an essential role of LRR1 in parasite survival.

In a continuing effort to characterize the regulators of PP1 in *P. falciparum*, a recent examination of its genome revealed the presence of a putative gene product encoded by PF10_0311 orf (designated in this study PfI3) that shared ~30% identity with Inhibitor-3 (I3 in mammals or Ypi1 in yeast), an essential regulator of PP1 expressed by different organisms (22, 23). In yeast, it has been shown that the deletion of Inhibitor-3 ortholog (*Ypi1*) is lethal for *Saccharomyces cerevisiae*, suggesting an essential function of the gene in the physiology of the yeast, and its depletion (conditional strain) affected the distribution of PP1 and provoked a blockage in anaphase with condensed chromosomes (24). Indirect evidence supporting the idea that Inhibitor-3 inhibits PP1 is the fact that overexpression of this regulator reduces glycogen levels in the yeast because glycogen synthase requires dephosphorylation by PP1 to become active (25). Here, we report the identification and characterization of PfI3 using biochemical, structural, and genetic approaches. Our results indicate the following. 1) PfI3 interacts *in vitro* directly with PfPP1, with high affinity. Unlike other I3s, this binding stimulates PfPP1 activity toward a nonspecific substrate defining PfI3 as a positive regulator of PfPP1. This could explain why PfI3 is not a functional ortholog of the yeast I3. 2) Detailed study of the interaction with complementary methods, including high resolution NMR spectroscopy, showed the importance of the conserved RV*X*F motif in mediating the binding to PfPP1. 3) Transfection experiments to obtain knock-out parasites strongly suggest its essentiality in blood parasite survival. 4) The generation of *PfI3-GFP* transgenic parasites revealed the PfI3 is mainly localized in the nucleus whatever the stage of the blood parasite, suggesting the regulation of PfPP1 in this compartment.

[5] J. Khalife, unpublished data.

EXPERIMENTAL PROCEDURES

Materials—Plasmids pQE30, pGEX4T3, pETDuet, and pACT2 were purchased from Qiagen, Life Sciences, Novagen, and Clontech, respectively. Plasmids pCAM-HA, pCAM-GFP, and pCAM were kind gifts from Dr. C. Doerig (Inserm-EPFL Joint Laboratory, Switzerland). GST-Ypi1 and GST-I3 recombinant proteins were prepared as described previously (25, 26) with pWS93 to tag proteins with HA_3 epitopes, and pBTM116 vectors for yeast two-hybrid experiments have been previously described (27, 28). Plasmid construction of pWS93-*Ypi1* has been described previously (25), and pBTM116-*Glc7* was generated by subcloning the BamHI fragment obtained by digestion of pGAD-Glc7 plasmid reported previously (29). The encoding region of *PfI3* amplified with primers P15 and P16 (supplemental Table 1), cloned initially in TA vector and sequenced, was cloned into BamHI-SalI sites and into EcoRI-SalI sites of pWS93 and PBTM116 vectors, respectively. With respect to *PfPP1*, the encoding region amplified with primers P17 and P18 (supplemental Table 1), initially cloned in pGBKT and sequenced, was cloned into EcoRI-BamHI sites and SfiI-XhoI sites of pBTM116 and pACT2 vectors, respectively. Monoclonal anti-HA and anti-Myc antibodies were purchased from Roche Applied Science and Invitrogen, respectively.

Preparation of Parasites—P. falciparum 3D7 clone was grown according to Trager and Jensen (30), in RPMI 1640 medium with 10% human AB^+ serum, in the presence of O^+ erythrocytes. Cultures were maintained at 37 °C in a humidified atmosphere (5% CO_2, 5% O_2, and 90% N_2). Parasites were synchronized by a double sorbitol treatment as described previously (31). To isolate total RNA or proteins, parasitized erythrocytes were lysed by saponin (32) and either resuspended in TRIzol (Invitrogen) or in phosphate-buffered saline containing EDTA-free protease inhibitor mixture (Roche Applied Science). For some experiments, infected red blood cells were purified using Percoll-sorbitol density gradients with slight modifications (33). Protein extracts were prepared from saponin-isolated parasites by resuspending the pellet in lysis buffer 1 (50 mM Tris-HCl, pH 7.4, 0.1% SDS, 0.05% sodium deoxycholate, and protease inhibitors mixture) or lysis buffer 2 (50 mM Tris, pH 7.4,150 mM NaCl, 20 mM $MgCl_2$, 1 mM EDTA, 1 mM DTT, 0.5% Triton X-100, 1% Nonidet P-40, and protease inhibitors mixture (Roche Applied Science)) followed by five consecutive freezing/thawing cycles with intermediate homogenizing steps using a micro-pestle and 0.7-mm glass beads (Sigma) and subsequent centrifugation at 13,000 rpm for 30 min at 4 °C.

Cloning of Full-size Open Reading Frame and Analysis of PfI3—All primers used throughout this study are listed in supplemental Table 1. The encoding region of *PfI3* was initially obtained from first strand cDNA derived from mRNA prepared from unsynchronized blood cultures of *P. falciparum* 3D7. The PCR was performed with the P1 and P2 primers using the Advantage 2 PCR kit (Clontech). To confirm the stop codon, 3′-rapid amplification of cDNA ends was carried out using the SMART kit (Clontech). The 3′ end was obtained using the forward primer F2 and the adapter primer according to the manufacturer's instructions. To determine the start codon, four forward

primers (P3, P4, P5, and P6) derived from the 5′ upstream genomic region were tested by PCR on cDNA with the reverse R2 primer derived from the coding region. P1 and P2 primers amplified one PCR product of the expected size. PCR products were cloned in TA cloning vector (Invitrogen) and sequenced. Comparative analysis of the PfI3 protein was performed by DNASTAR and ClustalW and using the Pfam database.

Generation of P. falciparum Transgenic Parasites—The *PfI3* disruption plasmid (pCAM-*PfI3*) was generated by inserting a PCR product corresponding to a 5′ portion from the *PfI3* sequence (550 bp) into the pCAM-BSD vector that contains a cassette conferring resistance to blasticidin. The insert was obtained using 3D7 genomic DNA as template and the oligonucleotides P29 and P20, which contain PstI and BamHI sites, respectively. Attempts to check the accessibility of the *PfI3* locus were performed by transfecting wild 3D7 parasites with 3′-tagging constructs. To this end, the 3′ end of the *PfI3* sequence (650 bp, omitting the stop codon) was amplified by PCR using 3D7 genomic DNA and the primers P21 and P22 containing PstI and BamHI restriction sites, respectively. The 3′-tagging plasmids were generated by inserting the PCR product into PstI and BamHI sites of the pCAM-BSD-hemagglutinin (HA) or GFP plasmids. Transfections were carried out by electroporation of ring stage 3D7 parasites with 75–100 μg of plasmid DNA, according to Sidhu *et al.* (34). To select transformed parasites, 48 h after transfection, blasticidin (Invivogen) was added to a final concentration 2.5 μg/ml. Resistant parasites appeared after 3–4 weeks and were maintained under drug selection. Populations of stably transfected parasites were obtained after 6 weeks. To enrich the populations for integrants, 3–4 cycles of on/off drug were applied.

Genotype and Phenotype Analysis of P. falciparum Transfectants—To confirm that transfected parasites contained the right constructs, plasmid rescue was carried out. Genomic DNA extracted (KAPA Express Extract, Kapa BioSystems) from wild or transfected parasites was used to transform *Escherichia coli* DH5α cells (Invitrogen). Plasmid DNA was then purified from bacterial clones and digested with PstI and BamHI. Genotypes of *PfI3* knock-out parasites were analyzed by PCR on genomic DNA using standard procedures with the primer numbers P27 (derived from the 5′-nontranslated region and not present in the construct) and P168 specific for the pCAM-BSD vector. Genotypes of *PfI3* knock-in were analyzed using the primer P29 and P639 or P635 (reverse primer corresponding to HA or GFP, respectively). The expression of PfI3-HA or -GFP fusion protein was checked by Western blotting. Live parasites potentially expressing PfI3-GFP were analyzed by fluorescence microscopy as described below.

Recombinant Protein Expression and Purification—The full-length coding region of *PfI3* obtained by PCR with the primers P7-P8 or P9-P10 was subcloned in pQE30 and pGEX4T3, respectively. For the expression of PfPP1 obtained with the primers P11 and P12, the pETDuet expression system was used. The restriction sites are mentioned in supplemental Table 1. Before cloning in expression vectors, all PCR products were subcloned in a TA cloning vector and verified by sequencing for the absence of any modification introduced by *Taq* polymerase. To obtain the *PfI3W45A* mutant construct, we performed a PCR-based site-directed mutagenesis strategy using the constructions pQE30-*PfI3* or *pGEX4T3-PfI3* as templates, the primers P13 and P14, and Isis Proofreading DNA polymerase (Qbiogene). The PCR conditions consisted of 30 s at 95 °C followed by 16 cycles at 95 °C (30 s), 50 °C (1 min), and 72 °C (5 min). The parental DNA plasmid was then digested with DpnI, and an aliquot was used to transform XL10-Gold ultracompetent cells (Stratagene). Mutated plasmids, checked by sequencing for the replacement of Trp^{45} by alanine, were used for the expression of the PfI3 W45A recombinant protein. Protein expression was carried out in the *E. coli* M15 strain for the pQE30 construct and the BL21 strain for pGEX4T3 and pET-Duet constructs. The expression of PfI3 and PfI3W45A was carried out in the presence of 1 mM isopropyl 1-thio-β-D-galactopyranoside at 37 °C for 3 h. For the expression of PfPP1, the culture was induced overnight at 16 °C in the presence of 0.5 mM isopropyl 1-thio-β-D-galactopyranoside and 2 mM $MnCl_2$. Cells were harvested in sonication buffer (50 mM Tris, pH 7.8, 1% Triton X-100, 1 mM DTT, and protease inhibitor mixture (Roche Applied Science)). His- or GST-tagged proteins were purified according to manufacturer's instructions by Ni^{2+} chelation chromatography or glutathione-agarose beads, respectively (Sigma). With respect to the PfI3-His protein, the extract was loaded on a 1-ml nickel-NTA resin column (HiTrap, GE Healthcare). Washing steps were performed with a buffer containing 50 mM sodium phosphate, pH 7.8, 300 mM NaCl, and 20 mM imidazole. Elution was done with a gradient from 50 to 250 mM imidazole. The eluted proteins were dialyzed against 50 mM Tris, pH 7.4, 150 mM NaCl. Under these conditions, the purity checked by SDS-PAGE followed by Coomassie Blue staining was >95%. The PfI3 recombinant protein was further subjected to peptide mass fingerprint by MALDI-TOF mass spectrometry as described previously (35). The resulting peptides matched with the sequences covering the amino acid positions are as follows: 42–57; 42–58; 45–57; 45–58; 71–93; 71–94; 101–115, and 102–116 confirming PfI3 identity.

Preparation of Isotope-labeled PfI3 Proteins and NMR Spectroscopy—M15 bacteria containing pQE30-*PfI3* or pQE30-*PfI3W45A* constructs were grown in minimal medium (M9) supplemented with $^{15}NH_4Cl$ (1 g/liter) and glucose (2 g/liter), ^{13}C-labeled or not, as the nitrogen and carbon sources, respectively. For the wild type protein, purification was performed by heating the cell extract for 15 min at 75 °C and centrifuging, followed by nickel-affinity chromatography (HiPrep Ni-NTA, GE Healthcare) on the supernatant. The purified protein was then exchange to 50 mM ammonium bicarbonate buffer, using a HiPrep desalting column (HR16/60, GE Healthcare) before lyophilization.

A slightly different protocol was used for the PfI3W45A protein. The first step of protein heating was skipped, and the nickel affinity-purified protein was directly exchanged against the NMR buffer (PD10, G-25 desalting resin, GE Healthcare) and concentrated using centrifugal devices. NMR buffer is 25 mM Tris-d_{11}, pH 6.8, 25 mM NaCl, 2.5 mM EDTA, 1 mM d_4-trimethylsilyl propionate as proton chemical shift internal reference, and 5% D_2O. Additionally, 1 mM of tri-(hydroxypropyl) phosphine was used as reductor in the three-dimensional experiments that required several days of data acquisition,

whereas 2.5 mM dithiothreitol (DTT) was used for two-dimensional {^{1}H,^{15}N}HSQC. Proteins in NMR buffer were at 250 μM for the three-dimensional experiment series and 100 μM for two-dimensional {^{1}H,^{15}N} HSQC. NMR spectra were recorded at 20 °C on a Bruker DMX600 spectrometer equipped with a triple resonance cryogenic probe head (Bruker, Karlsruhe, Germany). Classical pairs of three-dimensional HNCACB, HN(CO)CACB, HNCO, HN(CA)CO, and HN(CA)N were processed using Bruker TOPSPIN 2.1 and used for the assignment of the backbone ^1H_N, ^{15}N, and Cα atoms, and Cβ (supplemental Table S2). The backbone assignment is not complete due to weak signals in several regions of the protein (N terminus, Lys^{58}–Lys^{68} and Asp^{90}–Asn^{103}). For the assignment of the PfI3W45A mutant, only an additional pair of three-dimensional HNCACB and HN(CO)CACB was necessary. NMR mapping of the interaction of PfI3 (or PfI3W45A) with PfPP1 was performed by comparison of {^{1}H,^{15}N} HSQC spectra acquired with 2048 and 256 points in the direct and indirect dimensions, respectively. 64 scans were used for the control experiment with PfI3 (or PfI3W45A) alone (100 μM) and 256 scans for the interaction mapping experiment. The increased scan number in the latter case is necessary to compensate for dilution due to the addition of an equivalent volume of 100 μM PfPP1 in phosphatase buffer to half of the [^{15}N]PfI3 ([^{15}N]PfI3W45A) sample, resulting in an equimolar concentration of 50 μM each. To further ensure adequate comparison of these {^{1}H,^{15}N}HSQCs, intensities were normalized in each spectrum by the average value of the resonances of residues 110, 112, and 114 that are intense. Peak picking and intensity measurements were performed using Brüker TOPSPIN 2.1 software (Bruker, Germany). Secondary ^{13}Cα chemical shifts correspond to the difference between the experimental ^{13}Cα chemical shift value for each residue in the protein and the reference value for the corresponding amino acid residue found in databases of chemical shifts obtained from strictly disordered proteins or peptides. Secondary ^{13}Cα chemical shifts were here calculated as indicators for residual local secondary structure based on the random coil value database from Wishart *et al.* (36, 37), with a 2 ppm correction on the Cα value of residues with a Pro at the +1 position. The secondary structure propensity analysis compares the Cα and Cβ values not only to the random coil values expected in a strictly disordered protein but also to the Cα and Cβ values expected in a fully formed α-helix or β-strand, taking additionally into account the propensity of a given amino acid to adopt such a secondary structure. The results correspond for each amino acid residue to the fraction of the conformer distribution to adopt a secondary structure. Secondary structure propensity scores (38) were calculated using the refDB random coil database (39). Positive values of both secondary ^{13}Cα chemical shifts and structure propensity are related to an helical tendency, although negative values indicate an extended conformation.

GST Pulldown Assay and Immunoblot Assays—Preparation of recombinant proteins for pulldown assays was essentially as described above. Briefly, the *E. coli* extracts containing GST-PfI3 or GST-PfI3W45A (corresponding to a culture of 250 ml) were allowed to bind to glutathione beads overnight at 4 °C. Beads were then washed twice with PBS and twice with binding buffer (50 mM Tris-HCl, pH 8, 150 mM NaCl, 5 mM EDTA, 0.5% Nonidet P-40, and protease inhibitor mixture). The beads were then incubated for 45 min at room temperature under gentle rotation in 200 μl of binding buffer containing 25 μg of BSA and 10 μg of purified PfPP1. Beads were recovered by centrifugation, washed six times in the binding buffer, resuspended in SDS-PAGE buffer, and loaded on a 12% denaturing polyacrylamide gel. GST alone was used as a control. Proteins retained by the affinity column were detected by immunoblot using anti-GST or anti-His monoclonal antibodies.

Measurement of Binding of PfI3—Binding of recombinant PfI3 and PfI3W45A proteins to PfPP1 was assessed by an ELISA-based assay. Plates were coated with 100 μl per well at 10 μg/ml of either PfI3 or PfI3W45A protein in PBS overnight at 4 °C. Following washings with 0.1% PBS/Tween, the plates were blocked with PBS containing 0.5% gelatin for 1 h at room temperature. Coated plates were then incubated with different concentrations of biotinylated PfPP1 (labeled with biotin-NHS according to the manufacturer's instructions (Calbiochem)) in PBS/Tween 0.1% at 37 °C for 2 h. After five washes with 0.1% PBS/Tween, binding was detected using streptavidin-HRP. After a 30-min incubation and five washes, trimethylbenzidine substrate (Uptima) was added, and the reaction was stopped using 2 N HCl. The optical density was measured on an ELISA plate reader at 450 nm. In these experiments, BSA was used as control. The statistical significance was calculated with the Mann-Whitney *U* test for nonparametric data. p values < 0.05 were considered significant.

Surface Plasmon Resonance Experiment—The SPR binding studies were performed on a BIACORE 2000 instrument. The PfI3 protein was captured on a CM5 sensor chip using the amine coupling immobilization method according to the manufacturer's instructions (115 μl of 0.2 M 1-ethyl-3-(3-dimethylaminopropyl) carbodiimide mixed with 115 μl of 0.05 M *N*-hydroxysuccinimide to give reactive succinimide ester groups). PfI3 was diluted in 10 mM sodium acetate, pH 5, at a final concentration of 500 nM and injected, until a relative resonance unit (RU) of ~550 was reached. Remaining active groups were blocked by injection of 75 μl of 1 M ethanolamine, pH 8.5. The first flow channel of the sensor chip did not contain any immobilized ligand and served as a reference surface. The PfPP1 analyte was diluted in TBS buffer (pH 7.5, 100 μM $MnCl_2$) and injected over PfI3 at 30 μl/min for 3 min followed by a 15-min dissociation step. The surfaces were regenerated between binding cycles by one injection of 50 mM NaOH for 1 min. Binding curves were obtained over a range of analyte concentrations. A second CM5 sensorchip has been realized at a very low ligand immobilization (~200 RU). The data were analyzed, and association/dissociation constants were calculated using BIAevaluation 4.1 software (Biacore®, GE Healthcare).

Functional Complementation of S. cerevisiae—For the complementation assays, we constructed the conditional null mutant W303 *ypi1*Δ::*KANMX*4 (pGAL-HA-Ypi1), where the expression of *Ypi1* is under the control of the *GAL1* promoter. In this way, when the cells are grown in media with galactose as a carbon source they grow normally, and when they are shifted to media containing glucose as a carbon source they become unviable because they are *Ypi1*-depleted. This strain was trans-

formed with the plasmids indicated in the corresponding assay to overexpress different proteins and was grown during 3 days in media containing either galactose or glucose as carbon source. Standard methods for genetic analysis and transformation were used. Yeast cultures were grown in rich medium (YPD) or synthetic complete (SC) medium lacking the appropriate supplements to maintain selection for plasmids (40) containing the indicated carbon sources.

Assays for PfPP1 and Effect of PfI3—The activity of PfPP1 with *p*-nitrophenyl phosphate (pNPP) as substrate was assayed exactly as described previously (19). To investigate the role of PfI3 on PfPP1 activity, different amounts of PfI3 were added to PfPP1 and preincubated for 30 min at 37 °C before testing the PfPP1 phosphatase activity. The effect of GST, GST-I3, or GST-Ypi1 recombinant proteins was performed as described previously (25). Results are presented as mean of increase or decrease of phosphatase activity in comparison with PP1 incubated in the reaction buffer.

Localization of PfI3—For an episomal expression of PfI3-GFP, the full-length coding region of *PfI3* was amplified by PCR with the primers P22 and P23 containing XhoI and KpnI restriction sites, respectively. The PCR fragment was cloned into TOPO-TA cloning vector (Invitrogen), and its nucleotide sequence was verified. The PCR product was then subcloned in-frame with GFP into the pARL vector (kind gift of Dr. C. Sanchez, Heidelberg, Germany) (41) and digested with XhoI and KpnI. The plasmid carries the human *dhfr* gene for selection with WR99210. Populations of stably transfected parasites were obtained after 6 weeks. Live parasites were analyzed, and images were recorded by fluorescence microscopy (Zeiss, LSM710).

RESULTS

Molecular Cloning and Analysis of Pf Inhibitor-3—BlastP analysis of PlasmoDB using known Inhibitor-3 sequences allowed the identification of PF10_0311 as a *P. falciparum* homolog. Amplification of the open reading frame using cDNA obtained from total RNA of erythrocytic stages and primers mentioned under "Experimental Procedures" showed a PCR product with the expected size. This confirmed the transcription of PF10_0311 in blood parasite stages and confirmed the microarray data available in PlasmoDB. The cDNA sequence, designated *PfI3* in this work, confirmed the open reading frame (orf) predicted by PlasmoDB with only one different nucleotide at the position 263 (T → A), leading to a change of the amino acid sequence (Leu → Gln) (Fig. 1*A*). 3′-Rapid amplification of cDNA ends combined with a walking approach on cDNA from the 5′ side allowed the confirmation of the stop and start codons, respectively. As *P. falciparum* proteomic data revealed the presence of a peptide covering the sequence PMHSSSTTTTTTYVQDTNTQNDTNENSSTIVR (amino acid positions 3–34), it is very likely that the first methionine shown in Fig. 1*A* corresponds to the correct start codon of PfI3. The deduced amino acid sequence of the orf corresponds to a protein containing 116 amino acids with a predicted molecular mass of 13.1 kDa. The BLAST sequence analysis combined with visual inspection of PfI3 amino acid sequence showed 31% identity when compared with the human I3 (accession number CAC16920) and 28% with *S. cerevisiae* Ypi1 amino acid sequences (accession number NP_116658), respectively. However, the highest identity score (59 and 45% with the human and yeast counterparts, respectively) was found in the middle of the sequence between amino acids 39 and 81 (Fig. 1*B*). In this conserved sequence, we identified the motif KVVRW that corresponds to the PP1-binding motif R/K(X_1)$_{0-1}$(V/I)(X_2)(F/W), where X_1 and X_2 can be any amino acid except proline for X_2. It is important to note that the PP1-binding motif mentioned above fits with 90% of the known PP1-binding proteins described so far (42).

Expression of the PfI3 Gene Product by P. falciparum—To assess and to confirm the expression of the *PfI3* gene product in *P. falciparum*, we raised polyclonal antibodies against a recombinant His$_6$-PfI3 fusion protein (Fig. 2*A*). These antibodies were able to recognize the recombinant protein in Western blot analysis (Fig. 2*B*). The recombinant protein shared a molecular mass of around 20 kDa, in agreement with the anomalous electrophoretic behavior of I3 gene products of several species. However, immunoblot analysis using either soluble extracts from asynchronous erythrocytic parasites (20 μg per lane) or whole parasites solubilized in loading buffer (10^6 parasites per lane) did not allow the detection of PfI3 with these antibodies. This could be due to the quality/low affinity of produced antibodies and/or to the low level of expression of PfI3 by *P. falciparum*. Based on the view that PfI3 could be a partner of PfPP1, we attempted to perform affinity purification of endogenous PfI3 from whole parasite extract using His-tagged PfPP1 retained on Ni-NTA beads. As shown in Fig. 2*C, lane 2*, antibodies against recombinant PfI3 reacted with one band at 20 kDa, which corresponds to the SDS-PAGE migration of the recombinant PfI3. The presence of His-tagged PfPP1 in the eluted protein from the column was confirmed by the use of mAb anti-His antibody (Fig. 2*C, lane 3*).

Characterization of PfI3 Conformation in Solution Using NMR Spectroscopy—We used NMR spectroscopy to characterize the conformational properties of PfI3 in solution. Most of the ^{1}H,^{15}N signals of PfI3 in a two-dimensional-HSQC spectrum, corresponding to an amide group of an amino acid of PfI3, were assigned to a specific amino acid residue in the protein sequence using classical three-dimensional spectra of a doubly labeled [^{15}N,^{13}C]PfI3 (supplemental Table S2). Upon comparing the Cα chemical shift values of the PfI3 sample with the expected random coil values (36, 37), we can calculate the secondary Cα chemical shifts that are empirically correlated with the secondary structures (Fig. 3 and supplemental Fig. S1*A*). The Cα chemical shift values of PfI3 are close to the random coil values demonstrating the disordered nature of PfI3. A limited tendency to form secondary structure can however be observed in several segments of the protein. These structural elements remain in conformational exchange, as shown by the secondary chemical shifts that do not go beyond 1 ppm (supplemental Fig. S1*A*). Accordingly, the {^{1}H,^{15}N}HSQC spectrum of free [^{15}N]PfI3 shows the poor dispersion of the signals compatible with intrinsically disordered proteins (Fig. 4*A*).

A closer examination of the secondary Cα chemical shift values, performing a secondary structure propensity analysis (Fig. 3), reveals two major regions with helical propensity located

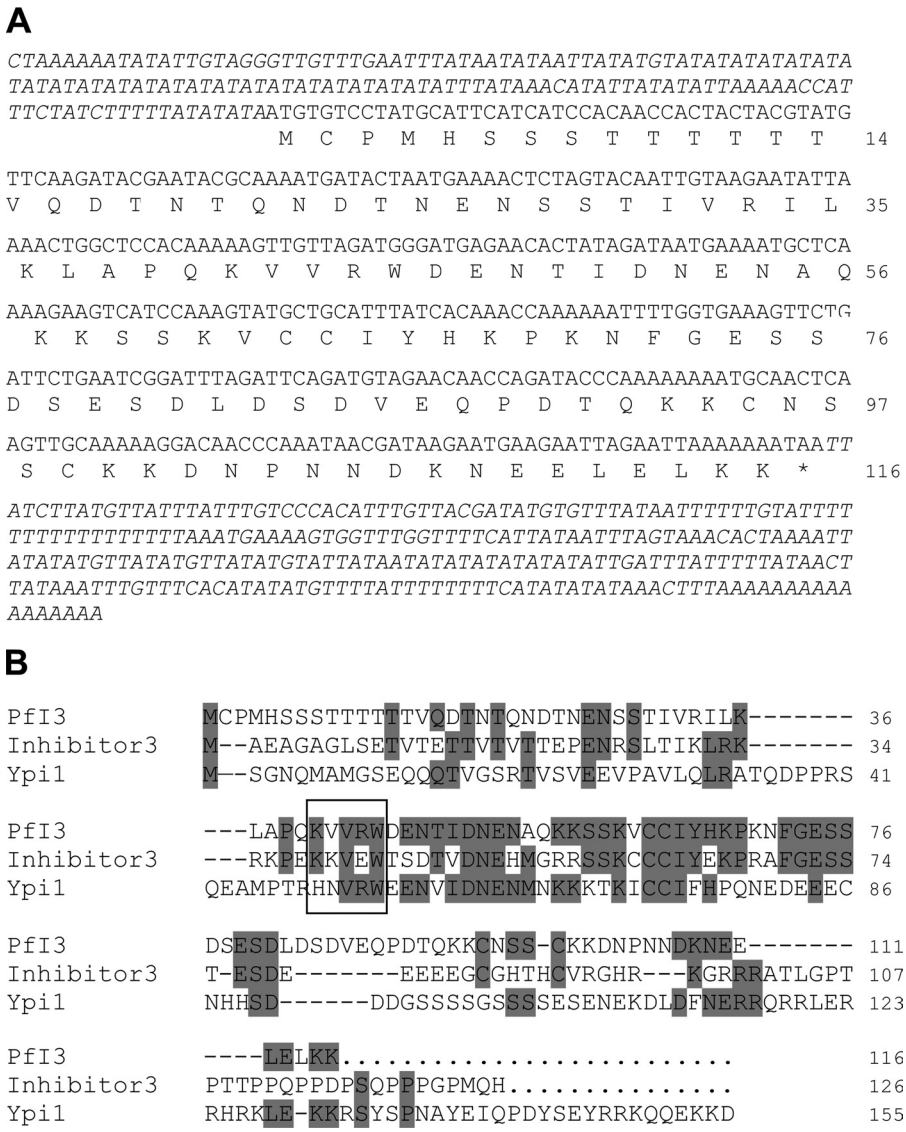

FIGURE 1. **Nucleotide and deduced amino acid sequences of PfI3.** *A,* amino acids are numbered to the *right* of the sequence. The sequences of 5′- and 3′-untranslated regions were obtained using primers derived from genomic DNA followed by PCR on cDNA and by performing 3′-rapid amplification of cDNA ends, respectively. *B,* analysis of amino acid sequence of PfI3. PfI3 was aligned with the mammalian (Inhibitor-3) and yeast I3 (Ypi1) homologs using the Megalign program (DNASTAR). The identical residues are shown in *gray*. The box contains the KVVRW sequence which fits with the consensus sequence (K/R)X_{0-1}(V/I)p(F/W), known as the RV*X*F motif and required for binding with PP1.

between residues Glu^{26}–Arg^{33} and Glu^{47}–Lys^{57} and two regions adopting preferentially the ϕ/ψ angles characteristics of extended conformations, Pro^{39}–Asp^{46} and His^{67}–Gly^{73}. A segment with helical tendency can additionally be confirmed at Asp^{90}–Cys^{95} by the Cα secondary chemical shifts (Fig. 3 and supplemental Fig. S1*A*). This analysis is corroborated by a PONDR prediction of the disordered regions of the PfI3 protein (43), based solely on the primary sequence, which shows a lower tendency for disorder (score <0.5) in regions Ser^{28}–Trp^{45}, Asn^{52}–Ser^{75}, and Gln^{92}–Pro^{104} (supplemental Fig. S1*B*).

Mapping of the PfPP1 Interaction Site(s) on PfI3 Using NMR Spectroscopy—We used {^{1}H,^{15}N}HSQC spectrum of PfI3 to map the interaction site with PfPP1, based on the assignment of the signals in this spectrum. Interaction indeed translates into a modification of the chemical shift and/or a broadening of the signals of those residues located in the interaction region as each {^{1}H,^{15}N}resonance is sensitive to the chemical environment of the corresponding residue. Comparison of {^{1}H,^{15}N}HSQC spectra of [^{15}N]PfI3, either free or in the presence of an equimolar amount of PfPP1, shows perturbations of numerous signals, which are broadened (Fig. 4*A*). This indicates a direct interaction between PfI3 and PfPP1. Comparison of the intensities of the signal along the protein sequence, between the free or bound PfI3 protein, allows the definition of a region of the protein Ser^{27}–Ser^{78} in which the corresponding resonances lose at least 50% of their intensity upon binding (Fig. 4*C*). This region includes the PfI3 sequence homologous to the PP1-binding site of yeast and human I3 containing the RV*X*F binding motif (KVVRW in PfI3). The two additional segments Thr^{12}–Gln^{16} and Lys^{93}–Asn^{103} show a decrease ratio of free *versus* bound resonance intensity, suggesting that they correspond to secondary binding sites of PfI3 to PfPP1.

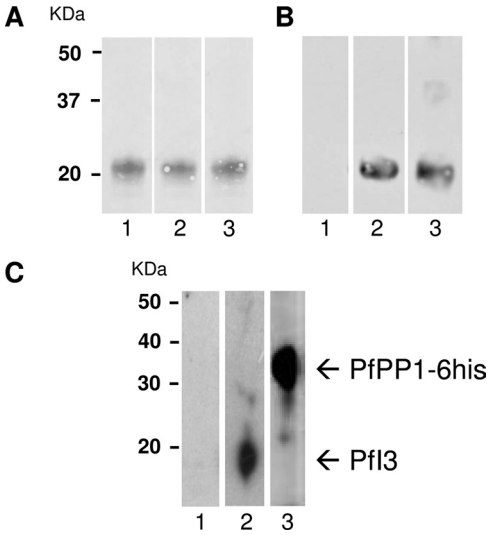

FIGURE 2. **Expression of the PfI3 gene product by *P. falciparum*.** *A,* purified His fusion PfI3 separated by 15% SDS-PAGE and blotted onto nitrocellulose (Red Ponceau staining, *lanes 1–3*). *B,* immunoblot analysis of recombinant PfI3 with rat prebleed sera (*lane 1*), with rat anti-PfI3 antisera (*lane 2*), and with mAb anti-His (*lane 3*) showed a single band at ~20 Da, indicating an anomalous electrophoretic migration of PfI3 (expected size 13 kDa). The identity of the purified recombinant PfI3 has been further confirmed by MALDI-TOF mass spectrometry. *C,* detection of endogenous PfI3 in total proteins extracted from asynchronous cultures of *P. falciparum*. Total protein extracts (10 mg) pre-cleared on Ni-NTA-Sepharose beads were incubated overnight with His_6-tagged PfPP1 affinity Ni-NTA column. After washings, proteins eluted with SDS-PAGE loading buffer were migrated and blotted to nitrocellulose. The blots were probed with preimmune serum (*lane 1*), anti-PfI3 (*lane 2*), or with anti-His mAb antibodies (*lane 3*). The blots were revealed as described under "Experimental Procedures."

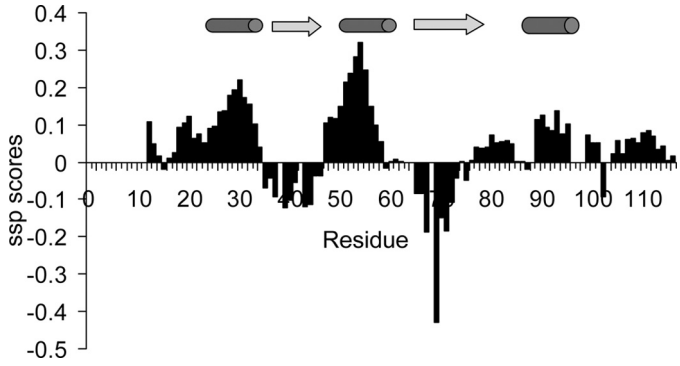

FIGURE 3. **Secondary structure propensity scores reported along the PfI3 sequence.** Positive values exceeding 0.1 are indicative of transient helices and negative values of extended transient conformations as represented by *cylinders* and *arrows* above the graphics, respectively.

To define whether the Trp residue of PfI3 is necessary for the binding or if the secondary sites that were defined by the above NMR analysis can interact independently, additional interaction mapping by NMR experiments were performed using this time a PfI3 protein containing an Ala residue in place of the Trp^{45}. Comparison of the two-dimensional $\{^1H,^{15}N\}$HSQC spectra of ^{15}N-labeled PfI3W45A and pfI3 shows that the resonances of the amino acid residues surrounding residue 45 have different chemical shifts, as expected for a point mutation (supplemental Fig. S2). Perturbations of the resonances in the PfI3W45A two-dimensional spectrum upon addition of a stoichiometric amount of PfPP1 were less important than observed for PfI3 (compare Fig. 4, *A* and *B*). From this result, and as expected from previous characterizations of the interaction of the PP1 phosphatase with several proteins, it seems that the region containing the RV*X*F motif is a major binding site with PfPP1. The intensity of each isolated resonance was compared in the HSQC spectrum of the bound, containing PfPP1, and free pfI3W45A samples (Fig. 4, *B* and *D*). Despite the absence of Trp^{45}, the analysis reveals several regions of interaction with PfPP1 characterized by decreased intensities and/or small chemical shift perturbations as follows: Ser^{29}–Gln^{40}, Lys^{61}–Lys^{70}, and Leu^{82}–Lys^{94} (Fig. 4, *B* and *D*). These regions correspond to the secondary interaction sites observed upon interaction of PfI3 and PfPP1. In contrast, the region of interaction surrounding the Trp^{45} does not interact with PfPP1 once the Trp is replaced by an Ala residue, as attested by the absence of chemical shift perturbation and/or intensity variation of the resonances of residues Gln^{40}–Ile^{50}. This additionally shows that the large interaction region defined in the wild type PfI3 protein as the main interaction site Ser^{29}–Ser^{75} can be divided into a central region surrounding Trp^{45} and two secondary binding sites Ser^{29}–Gln^{40} and Lys^{61}–Lys^{70} that bind independently.

Study of the Interaction between PfI3 and PfPP1—In vitro experiments were next performed to further examine the contribution of the RV*X*F motif of PfI3 for the binding to PfPP1. First, GST-pulldown experiments were carried out to explore the capacity of binding of recombinant PfI3 with PfPP1 and the contribution of the RV*X*F motif to this binding by use of the PfI3W45A mutant protein. Pulldown experiments followed by Western blot analysis (Fig. 5*A, upper panel*) showed that GST-PfI3 (*lane 2*) but not GST alone (*lane 1*) was able to bind efficiently to the recombinant PfPP1 protein. The pulldown experiments carried out with mutated PfI3 (PfI3W45A) revealed only a very faint band corresponding to PfPP1 when the Western blot was overexposed (Fig. 5*A*, *lane 3, upper panel*), suggesting that the interaction between PfI3 and PfPP1 was mainly due to the KVVRW motif. Loading controls with GST and GST-PfI3 are shown in the *lower panel* of Fig. 5*A*. Second, PfI3 and PfI3W45A were coated onto ELISA plates, and their binding capacity was examined using biotin-labeled PfPP1. Results presented in Fig. 5*B* evidenced the high capacity of PfPP1 to bind to PfI3, and the intensity of the signal was dependent on the amount of PfPP1 added. When PfI3W45A was coated, no significant binding to PfPP1 was observed, in accordance with the results obtained in the pulldown experiments. Based on the OD obtained and the quantity of PfPP1 added, it can be estimated that the KVVRW motif is the main contributor for PfI3 binding to PfPP1.

Next, we performed SPR measurement analysis (Biacore® 2000 system) to gain more insight on the PfPP1-PfI3 kinetic interaction. PfI3 was immobilized by amine coupling on a sensor chip (ligand), and increasing concentrations of PfPP1 were injected (analyte). Fig. 5*C* represents sensograms of a representative experiment out of three. Sensograms display an obvious association between PfI3 and PfPP1 that quickly achieves equilibrium. Dissociation occurs when running buffer without PfPP1 is switched. Biphasic nature of sensograms, clearly apparent when plotting the maximum response (RU max) reached for each concentration of analyte, suggests multiple

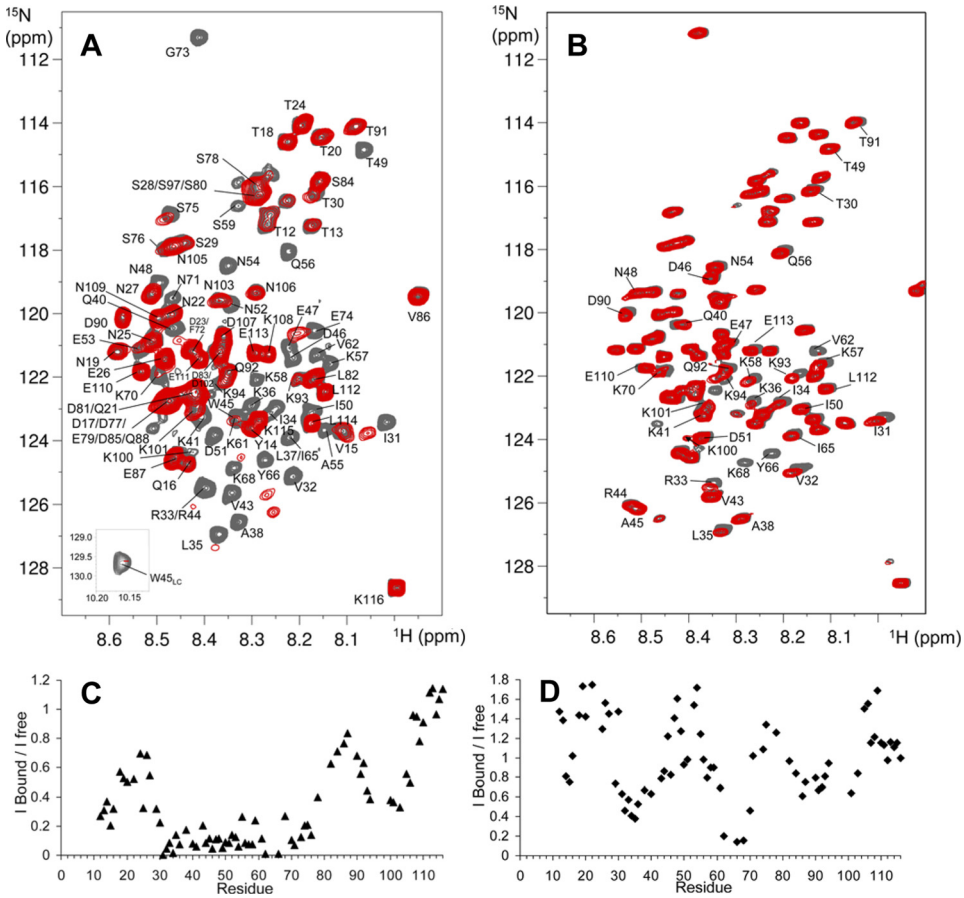

FIGURE 4. **NMR mapping of the PfI3 sites interacting with PfPP1.** *A*, overlaid {^{1}H-^{15}N} HSQC of ^{15}N-PfI3, free (*gray spectrum*), and in presence of an equimolar amount of PfPP1 (*superimposed red spectrum*). Interaction induces broadening of numerous resonances; see for example the isolated Gly^{73} resonance, in the *upper part* of the spectrum. The amide side chain resonance of Trp^{45} is shown as an *inset*. *B*, same color code is applied for the overlaid spectra corresponding to ^{15}N-PfI3W45A free or in presence of PfPP1. Resonances of PfI3 are all annotated (*A*), although the annotated resonances of ^{15}N-PfI3W45A are restricted to those showing perturbation upon PfPP1 addition or located around Ala^{45} (*B*). The supplemental Fig. S2 provides a comparison of the (^{1}H-^{15}N} HSQC of ^{15}N-PfI3 and ^{15}N-PfI3W45A. The graphics *below* the spectra show the normalized ratio of the intensity of a given resonance in the free PfI3 and in the 1:1 PfI3:PfPP1 spectra (*C*) or free PfI3W45A and in the 1:1 PfI3W45A:PfPP1 spectra (*D*), reported along the PfI3 sequence.

interaction sites between PfI3 and PfPP1 (Fig. 5*D*). Therefore, we can only extrapolate an apparent equilibrium constant K_D = 100 nM (BIAEvaluation 4.1). To confirm this observation, we performed additional experiments with a PfI3 low density binding on sensorchip that minimizes any potential steric hindrance or rebinding during dissociation (supplemental Fig. S3). SPR analysis indeed confirmed the existence of at least two binding sites with different affinities. These results suggesting the presence of primary high affinity (nanomolar) and secondary low affinity (micromolar) sites of interaction are in full agreement with the NMR experiments.

Genetic Manipulations of Inhibitor-3 in P. falciparum—Previous observations revealed that the deletion of Inhibitor-3 (*Ypi1*) demonstrated an essential function of this gene in yeast physiology. To investigate the role of the I3 ortholog in the *Plasmodium* life cycle, we attempted to disrupt the *PfI3* gene using the pCAM vector system (34). We transfected wild type 3D7 parasites with a plasmid containing a 5′ fragment derived from the genomic PfI3 sequence and the BSD gene, conferring resistance to blasticidin (Fig. 6*A*). We first attempted to detect the presence of the plasmid in transfected parasites by plasmid rescue. To this end, bacterial clones obtained after transformation with genomic DNA from blasticidin-resistant parasites were checked for the presence of the pCAM-BSD-*I3* plasmid. As shown in Fig. 6*C, lane 1*, resistant parasites carried the correct construct. However, genotype analysis by specific PCR of stable transfectant parasites (three independent transfection experiments) did not reveal the interruption of the gene (Fig. 6*D*). The wild type endogenous gene was still detectable in genomic DNA (Fig. 6*D*, *lane 1*). The plasmid remained episomal even after prolonged culture (>5 months of drug cycling, Fig. 6, *C*, *lane 1*, and *D*, *lane 2*). To check the accessibility for recombination of the genomic *PfI3* locus, we tried to modify the locus without causing loss-of-function of the gene product (Fig. 6*B*). We transfected wild type 3D7 parasites with a plasmid containing the 3′ end of the *PfI3* coding region fused to the hemagglutinin epitope. pCAM-PfI3-HA, blasticidin-resistant parasites, showed the presence of the correct construct (Fig. 6*C*, *lane 2*) and the integration of *PfI3-HA* into the *PfI3* locus (Fig. 6*E*, *lane 3*). Furthermore, Western blot analysis of these resistant parasites using mAb anti-HA antibody revealed the presence of a specific band at about 20 kDa (Fig. 6*F, lane 1*). Altogether these results indicate that the PfI3 locus is accessible to genetic manipulations. The unsuccessful attempts to recover *I3* KO parasites suggest that I3 is required for the completion of the cycle in red blood cells *in vitro*.

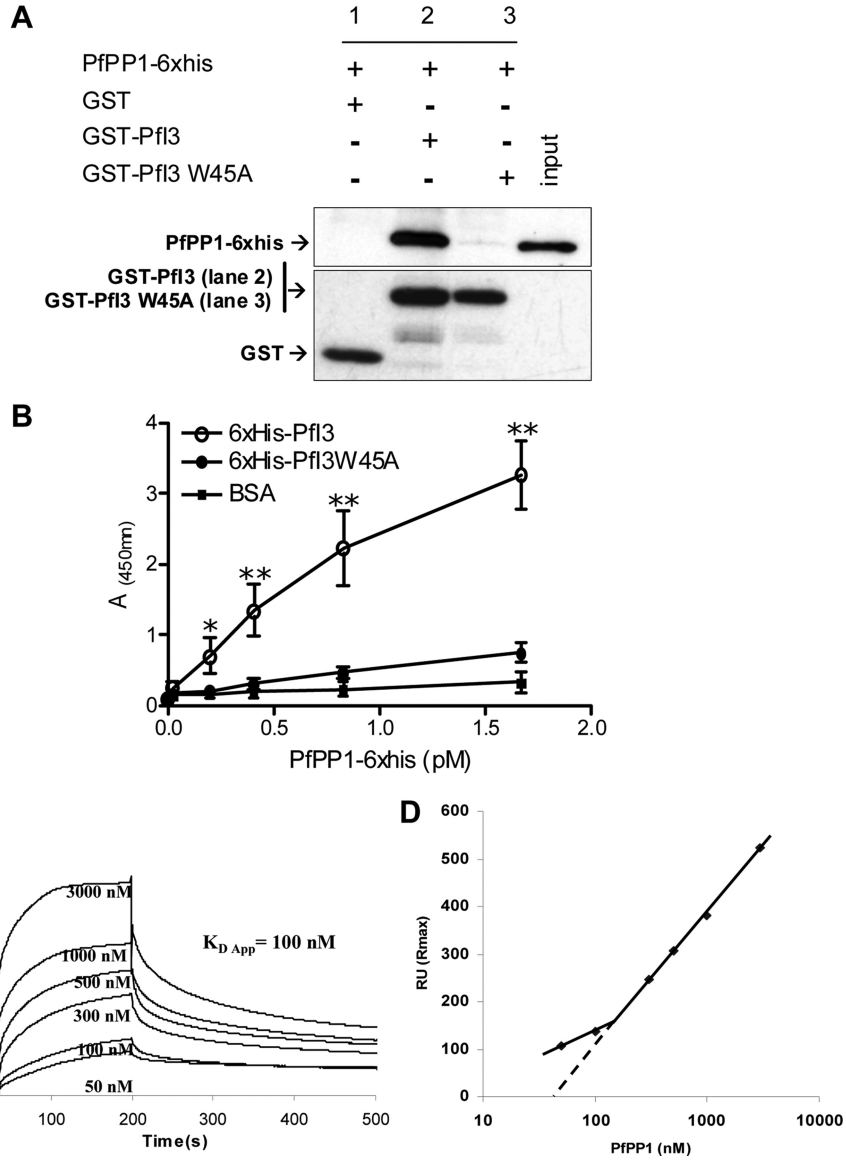

FIGURE 5. **Interaction studies of Pfl3 with PfPP1 *in vitro*.** *A,* GST-pulldown assays. Glutathione-agarose beads coupled with GST alone (*lane 1*), GST-Pfl3 bound to beads (*lane 2*), or GST-Pfl3W45A bound beads (*lane 3*) were incubated with His_6-tagged PfPP1. After washes, proteins bound to the beads were separated by 15% SDS-PAGE and blotted to nitrocellulose. Immunoblot analysis was performed with anti-His mAb (*upper blot*) and mAb anti-GST antibodies (*lower blot*) providing loading controls for bound GST and GST-fusion proteins. *B,* quantification of the binding capacity of PfPP1 to Pfl3 using an ELISA-based technique. Increased quantities of biotinylated PfPP1 were added to wells coated with recombinant Pfl3 or Pfl3W45A proteins (1 μg/well). Results represent experiments carried out with two different batches. *Bars* indicate S.E. ($n = 3$). *, $p < 0.05$; **, $p < 0.001$ when compared with either BSA or Pfl3W45A. *C,* surface plasmon resonance measurements. Pfl3 was immobilized on sensor chip, and increasing concentrations of PfPP1 (50–3000 nm) were used for injections. Base line of each sensogram was normalized and expressed in relative RU. Results shown are representative of three experiments. *D,* plot of the maximum RU reached in the experiment at each analyte concentration (log scale) shows a biphasic nature that can be explained by the presence of several binding sites of different affinities.

Study of Pfl3 Function Using the Yeast Model—The significant degree of similarity of yeast I3 (Ypi1) and Pfl3 prompted us to examine whether expression of *Pfl3* might rescue conditional *Ypi1*-depleted *S. cerevisiae*. First, we had to check whether Pfl3 was able to interact with the yeast PP1 (also known as the *GLC7* gene product) by yeast two-hybrid analysis. In these experiments, mammalian PP1α was also included. Unexpectedly and despite the sequence identity between all PP1s, >85% of Pfl3 did not show any interaction with mammalian PP1α as no β-Gal activity was detectable (Table 1). In contrast, the detection of β-Gal activity revealed an interaction of Pfl3 with both PfPP1 and Glc7 (Table 1). Based on this latter result, we next carried out experiments aimed at complementing a yeast strain deficient for Ypi1 expression. To this end, we constructed a *ypi1*Δ conditional yeast strain mutant where Ypi1 was expressed at physiological levels from a centromeric vector under the control of the p*GAL* promoter. In this way, cells were viable when growing in galactose-containing media but became unviable when cells were shifted to glucose-containing media. These cells were transformed either with empty vector (negative control), pWS93-HA-*Pfl3*, or pWS93-HA-*Ypi1*. Results presented in Fig. 7 show that the pWS93-HA-*Ypi1* construct was able to restore the growth of the *Ypi1*-depleted cells in glucose media (Fig. 7*C*). However, the pWS93-HA-*Pfl3* con-

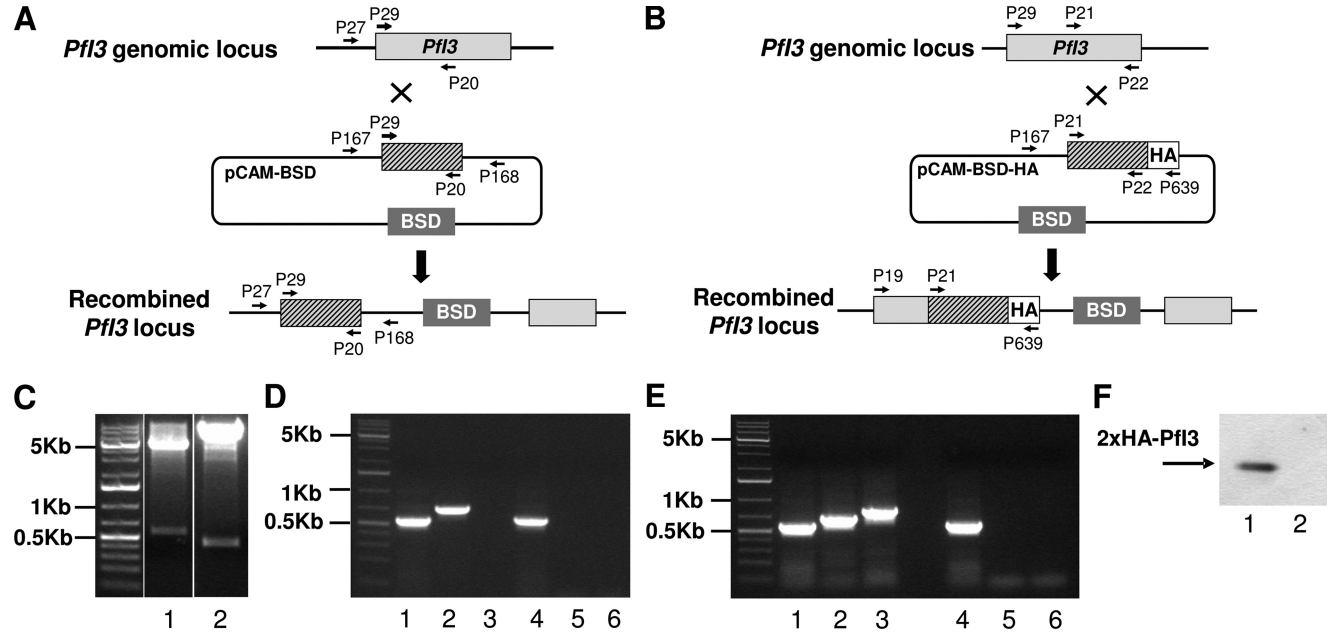

FIGURE 6. **Targeted gene disruption and HA tagging of the *Pfl3* locus.** *A,* gene-targeting construct for gene disruption by single homologous recombination using the pCAM-BSD, and the locus resulting from integration of the knock-out construct. *B,* epitope tagging of Pfl3 by knock-in strategy. Insertion of an HA epitope tag at the C terminus of *Pfl3* by single homologous recombination (knock-in). The locations of the primers (P29, P20, P21, P22, P27, P167, P168, and P639) used for PCR analysis are indicated as well as the blasticidin-resistance cassette (*BSD*). *C,* plasmid rescue experiments showing the presence of pCAM-Pfl3 (*lane 1*) and pCAM-Pfl3–2HA (*lane 2*) constructs in transfected parasite culture. *D,* analysis of pCAM-Pfl3-transfected 3D7 culture by PCR; *lanes 1–3* correspond to DNA extracted from transfected parasites; *lanes 4–6* correspond to DNA extracted from wild type parasites. *Lanes 1* and *4* represent the detection of a portion of the wild type locus (PCR with P29 and P20); *lanes 2* and *5* represent the detection of episomal DNA (PCR with P167 and P168); and *lanes 3* and *6* represent the detection of the integration at the 5′ end of the insert (PCR with P27 and P168). The absence of amplification of a PCR product using genomic DNA prepared from transfected parasite culture and using P27 and P168 as primers indicates the lack of homologous recombination (*lane 3*). *E,* analysis of pCAM-Pfl3–2HA transfected 3D7 culture by PCR; *lanes 1–3* correspond to DNA extracted from transfected parasites; *lanes 4–6* correspond to DNA extracted from wild type parasites. *Lanes 1* and *4* represent the detection of a portion of the wild type locus (PCR with P21 and P22); *lanes 2* and *5* represent the detection of episomal DNA (PCR with P167 and P639), and *lanes 3* and *6* represent the detection of the integration at the 3′ end of the insert (PCR with P29 and P639). The amplification of a PCR product at ~600 bp using genomic DNA prepared from transfected parasites indicates the homologous recombination and integration of the 2-HA tag construct in endogenous *Pfl3* (*lane 3*). *F,* immunoblot analysis of total extracts of transfected 3D7 with pCAM-BSD-Pfl3–2HA (*lane 1*) and wild 3D7 strain transfected (*lane 2*) 3D7 culture mAb anti-HA antibody.

TABLE 1

Interaction of PfI3 with PfPP1, yeast PP1 (Glc7), and human PP1α by yeast two-hybrid assay

β-Gal assay[a]	GAD	GAD-PfI3	GAD-PfPP1
LexA	−	−	−
LexA-PfPP1	−	+	
LexA-Glc7	−	+	
LexA-PP1α	−	−	
LexA-PfI3	−		+++
LexA-Ypi1	−		+++

[a] CTY.5d yeast strain was transformed with each pair of plasmids indicated in the table. The empty vectors (pBTM116 and pACT2) were used as controls. Transformants were grown on selective media plates and transferred to nitrocellulose filters to carry out β-galactosidase assays. At least six transformants of each pair were checked by this assay. The intensity of the interaction is specified as follows: −, no interaction; +, low interaction; +++, high interaction.

struct, like the empty vector, failed to rescue the same depleted strain. Western blots using extracts from transformed cells and mAb anti-HA antibody revealed that all strains tested expressed HA-*PfI3* or HA-*Ypi1* in similar amounts (Fig. 7*D*). These results suggest the possibility that PfI3 is nonfunctional in yeast, even though it binds yeast PP1, or that it fulfills a role distinct from that of Ypi1.

Effect of PfI3 on Phosphatase Activity of PfPP1—Many observations *in vitro* have defined Inhibitor-3 as a regulatory subunit of PP1 in plants, mammals, and yeast that acts by decreasing the activity of the latter against different nonspecific substrates, including myelin basic protein, phosphorylase *a*, or pNPP. Given that our results indicated that PfI3 was unable to complement the Ypi1-depleted yeast strain, although it could interact with Glc7 (Table 1), we investigated the effect of PfI3 on PfPP1 activity. No phosphatase activity could be detected with recombinant PfI3 alone when pNPP was used as substrate (data not shown). Unexpectedly, PfI3 strongly increased the dephosphorylation activity of PfPP1 in a concentration-dependent manner (Fig. 8, *A* and *B*). At all PfPP1 concentrations tested, the EC_{50} (effective concentration at which PfI3 confers 50% of maximal activation) value was less than 500 nM of PfI3. The same experiments were repeated with the PfI3W45A mutant, but we did not observe any change in the PfPP1 activity (Fig. 8, *A* and *B*). To provide convincing evidence that PfI3 is an activator of PP1, it was important to investigate whether the activity of PfPP1 could be decreased by known inhibitors. To this end, we examined the effect of human I3 and yeast Ypi1 proteins on PfPP1 phosphatase activity. As shown in Fig. 8*C*, both proteins inhibit the phosphatase activity reaching almost 70% inhibition (80% for Inhibitor-3) with the maximum amount assayed. Taking together all these data support the idea that the activation effect of PfI3 on PfPP1 phosphatase activity seems to be very specific and different from the mode of action of its mammalian and yeast homologs I3 and Ypi1.

Localization of PfI3—We next analyzed the localization of PfI3 protein in live 3D7 parasites transfected with the pARL2

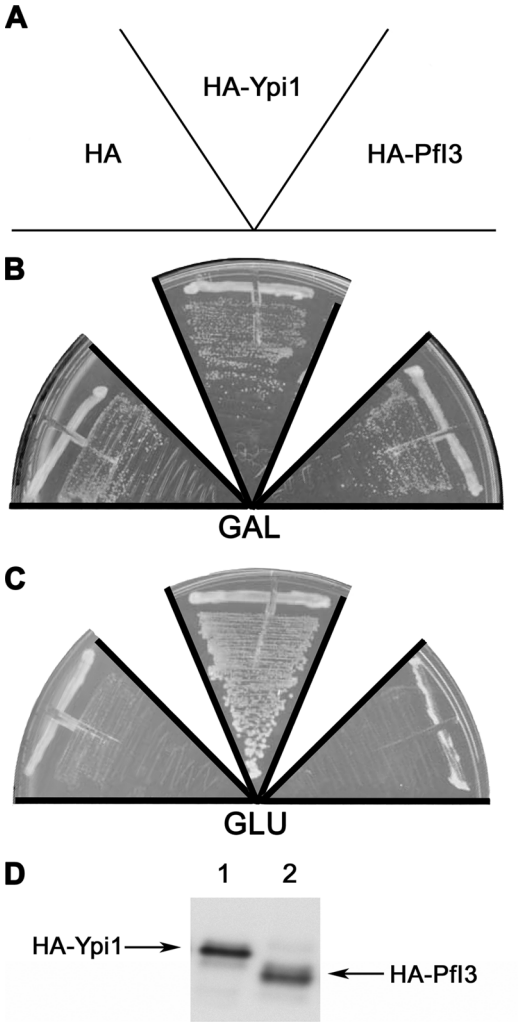

FIGURE 7. **Study of Pfl3 function using the yeast model.** Complementation assays using the conditional null *ypi*Δ mutant W303 *ypi1*Δ::*KANMX*4 (pGAL-HA-Ypi1) were done by transforming this strain with the plasmids expressing the proteins indicated in *A* (HA, pWS93; HA-Pfl3, pWS-Pfl3; HAYpi1, pWS-Ypi1). The transformants were grown during 3 days in selective media with galactose (*GAL*) (*B*) or glucose (*GLU*) (*C*). The figure is representative of the results obtained assaying at least four different transformants. Anti-HA immunoblot is representative of the expression of the HA-tagged Pfl3 or Ypi1 (*D*).

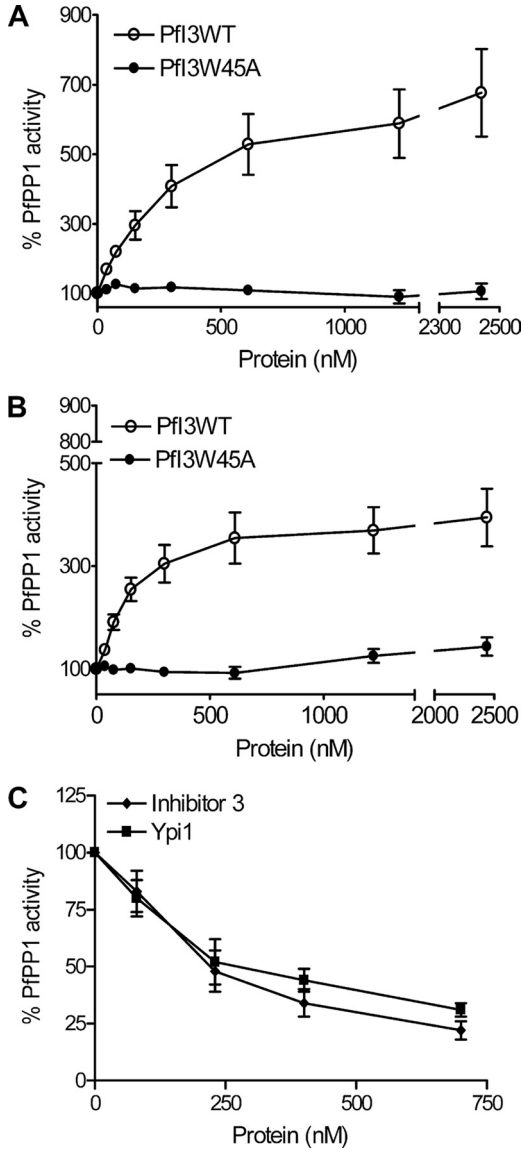

FIGURE 8. **Effect of Pfl3 and Pfl3W45 on PfPP1 phosphatase activity.** Recombinant PfPP1 at 71 nM (*A*) or at 143 nM (*B*) was preincubated for 30 min at 37 °C with different concentrations of Pfl3 or Pfl3W45A before the addition of pNPP. ○ represents the relative phosphatase activity in the presence of different concentrations of recombinant His_6-tagged Pfl3. ● represents the relative phosphatase activity in the presence of different concentrations of recombinant His_6-tagged Pfl3W45A. *C,* inhibition of PfPP1 phosphatase activity by human Inhibitor-3 and Ypi1. PfPP1 at 122 nM was preincubated for 10 min with different amounts of GST-Inh3 (♦) or GST-Ypi1(■) before the addition of pNPP. Results presented as % of relative increase or decrease are means ± S.E. for three independent experiments performed in duplicate.

construct mediating the expression of full-length GFP-fused *Pfl3* (Fig. 9*A*). It is important to mention that the use of this vector by Kuhn *et al.* (41) showed that the trafficking was attributed to the sequence of the protein *per se* rather than to the promoter used. The Pfl3 GFP-tagged protein was successfully expressed, and the integrity of the fused protein was maintained as observed by Western blot analysis (Fig. 9*C*). A single band with a molecular mass of 48 kDa was observed, which is the expected molecular mass of the GFP-tagged Pfl3. Examination of the localization of Pfl3 showed a distribution mainly in the nucleus of the parasite (Fig. 9*D*) as it is demonstrated by the overlap of DNA staining with the fluorescence of Pfl3-GFP. Examination of different parasite stages showed that the protein is imported into the nucleus of *P. falciparum* throughout the erythrocytic life cycle. Even at the very early stage (young ring), the expression of Pfl3 was observed in the nucleus (Fig. 9*D*).

DISCUSSION

PP1 belongs to the serine/threonine phosphatase family with representatives in animals (including helminth parasites), plants, and unicellular eukaryotes, including Apicomplexa, that share a high level of identity of amino acid sequences (>80%) (19, 21, 44). Several lines of evidence indicate that PP1 contributes to a wide range of physiological processes, including glycogen metabolism, smooth muscle contraction, and sperm motility (45–48). Further observations pointed out that PP1 also exerts important functions within the nucleus. It has been shown that PP1 participates in the control of transcription by interacting with RNA polymerase II and in a splicing process

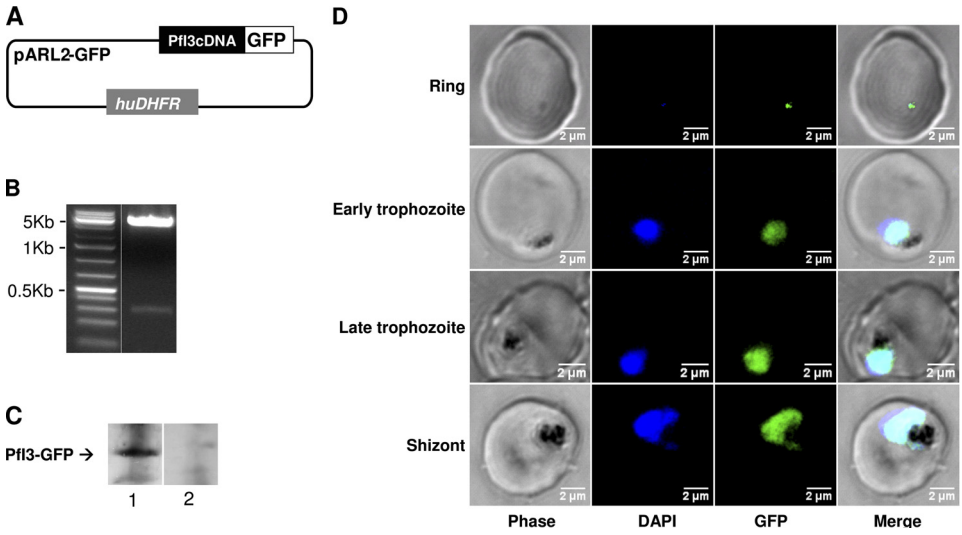

FIGURE 9. **Expression of Pfl3 gene products by transfected *P. falciparum*.** *A,* schematic representation of the pARL2-Pfl3-GFP used for episomal expression of Pfl3. The construct contains the complete open reading frame of Pfl3 in fusion with GFP. *B,* plasmid rescue experiments showing the presence of pARL2-Pfl3-GFP constructs in transfected parasite culture. *C,* immunoblot analysis of pARL2-Pfl3-GFP transfected *P. falciparum*. Proteins extracted from wild type parasites (*lane 1*) or from transfected parasites (*lane 2*) were subjected to Western blotting and probed with anti-GFP antibodies. *D,* expression and localization of Pfl3-GFP throughout the erythrocytic cell cycle of *P. falciparum.* Parasites were transfected as described under "Experimental Procedures," and live transfectants were analyzed by fluorescence microscopy.

(49–52). Moreover, it has been observed in many organisms that the impairment of PP1 activity leads to a mitotic arrest (53–57). Further studies have shown that PP1 activity should be closely controlled to ensure correct centrosome separation and for the segregation/decondensation of chromosomes (6, 58, 59). In *P. falciparum*, although it has been shown that PP1 is essential for parasite survival and for the release of infectious merozoites (12, 18, 60, 61), little is known about the expression of regulators of PP1 and on the nature of their exact functions. In this study, we have isolated a novel gene homolog to Inhibitor-3 (*I3*) of PP1, designated *Pfl3*, that has significant sequence identity with *I3* from a variety of organisms. Moreover, the inspection of its amino acid sequence revealed the presence of a KVVRW primary sequence that corresponds to the degenerate RV*X*F consensus sequence, identified as a binding motif to PP1 (22, 23, 25). To assess whether Pfl3 is a direct partner of PfPP1 and to map the Pfl3 protein interaction regions, purified recombinant [^{15}N]Pfl3 and PfPP1 were used in NMR spectroscopy experiments. This approach defined that the Pfl3 protein is mainly disordered in solution, in accordance with previous characterizations of other PP1-targeting proteins that were all shown to belong to the class of intrinsically disordered proteins (or partially disordered proteins) (62–66). The Pfl3 protein, however, shows in several regions a local tendency to fold into secondary structures. These transient conformations could fold upon binding, adopting stable secondary structures once in interaction with their protein partners (67). It is of interest to note that the combination of x-ray crystallography and NMR allowed us to show a significant role for the transient preformed structure in the interactions of several regulators with PP1 (62, 63, 68–71). Indeed, in Inhibitor 2, Spinophilin, and MYPT1 proteins, transient secondary structures characterized in the unbound states, were shown to be part of the interaction region and to be stabilized upon binding in the complex structure solved by crystallography (70, 71). With respect to the RV*X*F motif, found in an extended conformation in all the solved complexes of PP1, it also shows a tendency to adopt an extended conformation in the unbound state of MYPT1 (71). In the case of unbound Pfl3, we have also found that the region containing the RV*X*F motif Pro^{39}–Asp^{46} has a tendency for an extended conformation as well. This motif remains the main binding site as the replacement of Trp^{45} by an Ala residue will abolish binding of Pfl3 and PfPP1 as discussed below. Using the highly sensitive resonances of two-dimensional-HSQC spectra, we have additionally shown that besides this main binding site of Pfl3 to PfPP1, several secondary binding sites can be defined. These mapped secondary binding sites encompass transient secondary structures, like the binding region Lys^{61}–Lys^{70} that matches an extended tendency in the His^{67}–Gly^{73} segment or binding region Leu^{82}–Lys^{94} that corresponds to a helical tendency defined in Asp^{90}–Cys^{95} segment. It could thus well be the case that these local transient structures, defined using NMR parameters, reflect the bound conformation of Pfl3 with PfPP1. Despite the weaker affinity, the secondary binding sites are independent of the binding of the conserved region surrounding Trp^{45} as they can be detected in the Pfl3 mutant protein in which Trp^{45} has been replaced by an Ala residue. It was similarly recently proposed in the case of the interaction of human PP1 with the protein Myt1 that secondary binding elements of interaction, besides the conserved RV*X*F motif, could play a role as interaction anchors, positioning the interacting partners before formation of a tighter complex mediated by the RV*X*F motif.

The physical interaction between Pfl3 and PfPP1 was confirmed by GST pulldown assays and ELISA, and an apparent K_D value was determined by SPR analysis, confirming a strong interaction between partners. Analysis of fitting models suggests a complex interaction between PfPP1 and Pfl3, which involves at least two binding sites. These observations are in accordance with NMR studies presented in this work. They also

agree with several crystal structures of human PP1 complexes that show multiple sites of attachment, including Inhibitor-2 that belongs to the same family as Inhibitor-3 (69). Most importantly, mutation of the putative KVVRW motif present in PfI3 by substitution of Trp^{45} by Ala almost completely abolished the interaction between PfI3 and PfPP1. The results presented in this work suggest that the RV*X*F motif functions as a primary anchor to PfPP1, subsequently promoting the interaction of secondary binding sites, which can explain the observed NMR spectra. Our data concerning the implication of the RV*X*F motif are in agreement with previous binding data from both yeast and plant cells (22, 25), which revealed that this motif is critically required in PP1 binding. Regarding the region of PP1 involved in this interaction, structural studies of co-crystallized human PP1 and a peptide containing the RV*X*F motif demonstrated that the motif binds to a hydrophobic channel constituted by β-sheets within the *Ct* region of PP1 (72). Furthermore, the substitution of the phenylalanine residue of the binding motif by alanine abrogated the ability of the peptide to interact with PP1. Interestingly, the critical amino acids identified in the β-sheet conformation of mammalian PP1 are conserved in the sequence of PfPP1 (12).

The detection of the expression of the *PfI3* gene product by *P. falciparum,* attempted by direct Western blot assays with total parasite extracts, did not show any specific band using antisera raised against the recombinant protein. However, PfPP1 was able to pull down endogenous PfI3 from parasite extract, clearly showing its expression by blood stage parasites. To evaluate PfI3 function(s) in *P. falciparum*, disruption of the corresponding gene was investigated. Although stable transfectants were obtained, no mutants could be selected with a disrupted *PfI3* locus. The absence of knock-out parasites was not due to the inaccessibility of its locus for genetic modifications as we were able to obtain knock-in parasites expressing HA tagged PfI3. These data suggest that PfI3 is essential for blood stage parasites and are in agreement with the *in vivo* functional studies of I3 in other organisms that demonstrated the indispensable role of I3 in cell survival and division. Studies carried out in yeast showed that the deletion of *I3* (*Ypi1*) is lethal, and its conditional suppression leads to the inhibition of cell growth of mid-mitosis (24, 25). More recently, genetic studies in *Arabidopsis thaliana* revealed that *I3* disruption delayed the progression of embryogenesis and arrested the development at an early stage. In addition, the reduction of *I3* expression by RNA interference led to a significant decrease in fertility (22). Unfortunately, all attempts we made to induce RNA interference responses in *P. falciparum* have so far been unsuccessful (data not shown). To further examine the role of PfI3, we decided to determine whether it could function in yeast because both PP1 and I3 are highly conserved in this organism. We therefore used a conditional yeast strain deficient in the expression of I3 (*Ypi1* gene product). Heterologous complementation experiments using *PfI3* did not allow recovery of the growth of deficient yeast, although homologous complementation did rescue the same strain. The absence of recovery did not seem to be related to a defect in the interaction of PfI3 with yeast PP1. Our observation supports the idea that the PfI3-yeast PP1 complex is not able to fulfill similar functions such as those accomplished by the homologous yeast complex and suggests that the action of I3 on PP1 in *P. falciparum* may be different from those described in other eukaryotes. The failure to generate *P. falciparum* mutants with a disrupted *PfI3* locus is not absolute proof of the essential nature of the PfI3 protein, and additional approaches are required. A few *Plasmodium* conditional protein expression systems have been reported, but none of these have been proven to be reproducible for regulating *Plasmodium* protein expression (61, 73).

It has been shown that human, plant, and yeast I3 were able to regulate PP1 *in vitro* by inhibiting its activity toward different nonspecific substrates, including phosphorylase *a*, pNPP, or myelin basic protein (22, 23, 25, 74). To further assess the regulatory role of PfI3, we determined whether the PfPP1 activity could be influenced by PfI3. In a previous study, we showed that recombinant PfPP1 is catalytically active and can hydrolyze pNPP (19). Surprisingly, the inclusion of PfI3 at nanomolar concentrations to the reaction significantly increased the PfPP1 activity. This increase did not occur when PfI3 was replaced by mutated PfI3W45A, indicating the importance of Trp^{45} not only in the binding of PfI3 but also in the control of PP1 activity. Under the same conditions, the use of a mammalian I3 and yeast Ypi1 proteins significantly decreased the activity of PfPP1, ruling out any methodological artifact. Most importantly, these results indicate that, at least *in vitro*, PfI3 has opposite and specific effects on PfPP1 compared with other Inhibitor-3 homologs. However, precautions should be taken in drawing conclusions concerning the *in vivo* role of I3 in *P. falciparum,* and the determination of its exact function will await the further development of optimized conditional mutagenesis systems and the identification of nuclear substrate(s).

Having shown the ability of PfI3 to bind to PfPP1 and to regulate its activity, we next explored the localization of PfI3 by expressing it in *P. falciparum* as a fusion protein with a fluorescent reporter molecule. Interestingly, fluorescence microscopy of parasites transfected with PfI3-GFP construct revealed a specific localization that overlapped DNA staining, clearly pointing to a nuclear localization of PfI3 (Fig. 8). Examinations of blood parasites at different stages of growth demonstrated that there is no variation during the parasite cycle in its nuclear localization. These findings are in accordance with those reported for yeast where I3 was shown to be localized in the nucleus, like its PP1 partner (75). Our previous studies, using the subcellular fractionation of blood parasites, allowed the detection of PfPP1 both in cytoplasm and nuclear extracts (19). Together, these observations suggest that PfI3 could have a modulatory effect on PfPP1 activity toward nuclear substrates.

The findings reported in this study combined with previous observations on the expression of a second potential nuclear regulator (PfLRR1) of PfPP1, which we identified as a negative regulator (19), suggest that the regulation of PfPP1 must be coordinated and tightly controlled in the nucleus of *P. falciparum*. It is worthy of note that converging studies evidenced a major role for PP1 and its regulators in mitosis of many organisms (76). Recent work by Wu *et al.* (77) on HeLa and *Xenopus* cells suggests the implication of PP1 in a framework in which PP1 is blocked by inhibitor-1 during metaphase and a subsequent activation of PP1 ensuring the completion of mitosis.

Based on the view that any anomaly of PP1 activity in eukaryotic cells affects spindle organization and nuclear separation with overcondensed chromosomes, it seems very likely that the dephosphorylation of nuclear proteins directly or indirectly involved in molecular motors is vital and dynamically governed by PP1-regulator complexes. This is line with the fact that our attempts to express PfPP1-GFP episomally were unsuccessful (two different transfections, data not shown), supporting the conclusion that blood parasites are unable to accept exogenous expression of PfPP1 and any potential changes in the level of its activity.

Further studies will evaluate the ability of small molecules targeting the interface of interaction of PfPP1-PfI3 to follow up the phenotype of treated parasites. These explorations may help not only in deciphering the function of PfI3 but also in identifying inhibitors that can participate in a new strategy for drug discovery against malaria.

Acknowledgments—We thank Drs. Edith Browaeys, Katia Cailliau, Guy Lippens, and Jean-Michel Wieruszeski for helpful discussions; Dr. Raymond Pierce for the critical reading of the manuscript, and Claude Godin and Hervé Drobecq for technical assistance. The NMR facilities were funded by the Région Nord, CNRS, Pasteur Institute of Lille, European Community (FEDER), French Research Ministry, and the University of Sciences and Technologies of Lille I.

REFERENCES

1. Berndt, N. (1999) Protein dephosphorylation and the intracellular control of the cell number. *Front. Biosci.* **4,** D22–D42
2. Honkanen, R. E., Zwiller, J., Moore, R. E., Daily, S. L., Khatra, B. S., Dukelow, M., and Boynton, A. L. (1990) Characterization of microcystin-LR, a potent inhibitor of type 1 and type 2A protein phosphatases. *J. Biol. Chem.* **265,** 19401–19404
3. Ohta, T., Sueoka, E., Iida, N., Komori, A., Suganuma, M., Nishiwaki, R., Tatematsu, M., Kim, S. J., Carmichael, W. W., and Fujiki, H. (1994) Nodularin, a potent inhibitor of protein phosphatases 1 and 2A, is a new environmental carcinogen in male F344 rat liver. *Cancer Res.* **54,** 6402–6406
4. Sugiyama, H., Papst, P., Fujita, M., Gelfand, E. W., and Terada, N. (1997) Overexpression of wild type p70 S6 kinase interferes with cytokinesis. *Oncogene* **15,** 443–452
5. Cheng, A., Kaldis, P., and Solomon, M. J. (2000) Dephosphorylation of human cyclin-dependent kinases by protein phosphatase type 2C α and β2 isoforms. *J. Biol. Chem.* **275,** 34744–34749
6. Sassoon, I., Severin, F. F., Andrews, P. D., Taba, M. R., Kaplan, K. B., Ashford, A. J., Stark, M. J., Sorger, P. K., and Hyman, A. A. (1999) Regulation of *Saccharomyces cerevisiae* kinetochores by the type 1 phosphatase Glc7p. *Genes Dev.* **13,** 545–555
7. Watanabe, T., Ono, Y., Taniyama, Y., Hazama, K., Igarashi, K., Ogita, K., Kikkawa, U., and Nishizuka, Y. (1992) Cell division arrest induced by phorbol ester in CHO cells overexpressing protein kinase C-δ subspecies. *Proc. Natl. Acad. Sci. U.S.A.* **89,** 10159–10163
8. Wheatley, S. P., Hinchcliffe, E. H., Glotzer, M., Hyman, A. A., Sluder, G., and Wang, Y. (1997) CDK1 inactivation regulates anaphase spindle dynamics and cytokinesis *in vivo*. *J. Cell Biol.* **138,** 385–393
9. Bollen, M., Peti, W., Ragusa, M. J., and Beullens, M. (2010) The extended PP1 toolkit. Designed to create specificity. *Trends Biochem. Sci.* **35,** 450–458
10. Fardilha, M., Esteves, S. L., Korrodi-Gregório, L., da Cruz e Silva, O. A., and da Cruz e Silva, F. F. (2010) The physiological relevance of protein phosphatase 1 and its interacting proteins to health and disease. *Curr. Med. Chem.* **17,** 3996–4017
11. Hendrickx, A., Beullens, M., Ceulemans, H., Den Abt, T., Van Eynde, A., Nicolaescu, E., Lesage, B., and Bollen, M. (2009) Docking motif-guided mapping of the interactome of protein phosphatase-1. *Chem. Biol.* **16,** 365–371
12. Bhattacharyya, M. K., Hong, Z., Kongkasuriyachai, D., and Kumar, N. (2002) *Plasmodium falciparum* protein phosphatase type 1 functionally complements a glc7 mutant in *Saccharomyces cerevisiae*. *Int. J. Parasitol.* **32,** 739–747
13. Dobson, S., Bracchi, V., Chakrabarti, D., and Barik, S. (2001) Characterization of a novel serine/threonine protein phosphatase (PfPPJ) from the malaria parasite, *Plasmodium falciparum*. *Mol. Biochem. Parasitol.* **115,** 29–39
14. Dobson, S., May, T., Berriman, M., Del Vecchio, C., Fairlamb, A. H., Chakrabarti, D., and Barik, S. (1999) Characterization of protein Ser/Thr phosphatases of the malaria parasite, *Plasmodium falciparum*. Inhibition of the parasitic calcineurin by cyclophilin-cyclosporin complex. *Mol. Biochem. Parasitol.* **99,** 167–181
15. Li, J. L., and Baker, D. A. (1997) Protein phosphatase β, a putative type-2A protein phosphatase from the human malaria parasite *Plasmodium falciparum*. *Eur. J. Biochem.* **249,** 98–106
16. Li, J. L., and Baker, D. A. (1998) A putative protein serine/threonine phosphatase from *Plasmodium falciparum* contains a large N-terminal extension and five unique inserts in the catalytic domain. *Mol. Biochem. Parasitol.* **95,** 287–295
17. Mamoun, C. B., Sullivan, D. J., Jr., Banerjee, R., and Goldberg, D. E. (1998) Identification and characterization of an unusual double serine/threonine protein phosphatase 2C in the malaria parasite *Plasmodium falciparum*. *J. Biol. Chem.* **273,** 11241–11247
18. Yokoyama, D., Saito-Ito, A., Asao, N., Tanabe, K., Yamamoto, M., and Matsumura, T. (1998) Modulation of the growth of *Plasmodium falciparum in vitro* by protein serine/threonine phosphatase inhibitors. *Biochem. Biophys. Res. Commun.* **247,** 18–23
19. Daher, W., Browaeys, E., Pierrot, C., Jouin, H., Dive, D., Meurice, E., Dissous, C., Capron, M., Tomavo, S., Doerig, C., Cailliau, K., and Khalife, J. (2006) Regulation of protein phosphatase type 1 and cell cycle progression by PfLRR1, a novel leucine-rich repeat protein of the human malaria parasite *Plasmodium falciparum*. *Mol. Microbiol.* **60,** 578–590
20. Ohkura, H., and Yanagida, M. (1991) S. pombe gene sds22$^+$ essential for a midmitotic transition encodes a leucine-rich repeat protein that positively modulates protein phosphatase-1. *Cell* **64,** 149–157
21. Daher, W., Oria, G., Fauquenoy, S., Cailliau, K., Browaeys, E., Tomavo, S., and Khalife, J. (2007) A *Toxoplasma gondii* leucine-rich repeat protein binds phosphatase type 1 protein and negatively regulates its activity. *Eukaryot. Cell* **6,** 1606–1617
22. Takemiya, A., Ariyoshi, C., and Shimazaki, K. (2009) Identification and functional characterization of Inhibitor-3, a regulatory subunit of protein phosphatase 1 in plants. *Plant Physiol.* **150,** 144–156
23. Zhang, J., Zhang, L., Zhao, S., and Lee, E. Y. (1998) Identification and characterization of the human HCG V gene product as a novel inhibitor of protein phosphatase-1. *Biochemistry* **37,** 16728–16734
24. Pedelini, L., Marquina, M., Ariño, J., Casamayor, A., Sanz, L., Bollen, M., Sanz, P., and Garcia-Gimeno, M. A. (2007) YPI1 and SDS22 proteins regulate the nuclear localization and function of yeast type 1 phosphatase Glc7. *J. Biol. Chem.* **282,** 3282–3292
25. García-Gimeno, M. A., Muñoz, I., Ariño, J., and Sanz, P. (2003) Molecular characterization of Ypi1, a novel *Saccharomyces cerevisiae* type 1 protein phosphatase inhibitor. *J. Biol. Chem.* **278,** 47744–47752
26. Lesage, B., Beullens, M., Pedelini, L., Garcia-Gimeno, M. A., Waelkens, E., Sanz, P., and Bollen, M. (2007) A complex of catalytically inactive protein phosphatase-1 sandwiched between Sds22 and Inhibitor-3. *Biochemistry* **46,** 8909–8919
27. Song, W., and Carlson, M. (1998) Srb/mediator proteins interact functionally and physically with transcriptional repressor Sfl1. *EMBO J.* **17,** 5757–5765
28. Vojtek, A., Cooper, J., and Hollenberg, S. (1997) in *The Yeast Two-hybrid System* (Bartley, P., and Fields, S., eds) pp. 26–42, Oxford University Press, New York
29. Tu, J., and Carlson, M. (1995) REG1 binds to protein phosphatase type 1 and regulates glucose repression in *Saccharomyces cerevisiae*. *EMBO J.* **14,** 5939–5946

30. Trager, W., and Jensen, J. B. (1976) Human malaria parasites in continuous culture. *Science* **193,** 673–675
31. Vernes, A., Haynes, J. D., Tapchaisri, P., Williams, J. L., Dutoit, E., and Diggs, C. L. (1984) *Plasmodium falciparum* strain-specific human antibody inhibits merozoite invasion of erythrocytes. *Am. J. Trop. Med. Hyg.* **33,** 197–203
32. Umlas, J., and Fallon, J. N. (1971) New thick-film technique for malaria diagnosis. Use of saponin stromatolytic solution for lysis. *Am. J. Trop. Med. Hyg.* **20,** 527–529
33. Ginsburg, H., Landau, I., Baccam, D., and Mazier, D. (1987) Fractionation of mouse malarious blood according to parasite developmental stage, using a Percoll-sorbitol gradient. *Ann. Parasitol. Hum. Comp.* **62,** 418–425
34. Sidhu, A. B., Valderramos, S. G., and Fidock, D. A. (2005) pfmdr1 mutations contribute to quinine resistance and enhance mefloquine and artemisinin sensitivity in *Plasmodium falciparum*. *Mol. Microbiol.* **57,** 913–926
35. Rocha-Perugini, V., Montpellier, C., Delgrange, D., Wychowski, C., Helle, F., Pillez, A., Drobecq, H., Le Naour, F., Charrin, S., Levy, S., Rubinstein, E., Dubuisson, J., and Cocquerel, L. (2008) The CD81 partner EWI-2wint inhibits hepatitis C virus entry. *PLoS One* **3,** e1866
36. Wishart, D. S., and Sykes, B. D. (1994) The ^{13}C chemical-shift index. A simple method for the identification of protein secondary structure using ^{13}C chemical-shift data. *J. Biomol. NMR* **4,** 171–180
37. Wishart, D. S., Bigam, C. G., Holm, A., Hodges, R. S., and Sykes, B. D. (1995) ^{1}H, ^{13}C, and *15*N random coil NMR chemical shifts of the common amino acids. I. Investigations of nearest-neighbor effects. *J. Biomol. NMR* **5,** 67–81
38. Marsh, J. A., Singh, V. K., Jia, Z., and Forman-Kay, J. D. (2006) Sensitivity of secondary structure propensities to sequence differences between α- and γ-synuclein. Implications for fibrillation. *Protein Sci.* **15,** 2795–2804
39. Zhang, H., Neal, S., and Wishart, D. S. (2003) RefDB. A database of uniformly referenced protein chemical shifts. *J. Biomol. NMR* **25,** 173–195
40. Rose, M. D., Winston, F., and Hieter, P. (1990) in *Methods in Yeast Genetics: A Laboratory Course Manual*, Cold Spring Harbor Laboratory Press, Cold Spring Harbor, NY
41. Kuhn, Y., Sanchez, C. P., Ayoub, D., Saridaki, T., van Dorsselaer, A., and Lanzer, M. (2010) Trafficking of the phosphoprotein PfCRT to the digestive vacuolar membrane in *Plasmodium falciparum*. *Traffic* **11,** 236–249
42. Wakula, P., Beullens, M., Ceulemans, H., Stalmans, W., and Bollen, M. (2003) Degeneracy and function of the ubiquitous RV*X*F motif that mediates binding to protein phosphatase-1. *J. Biol. Chem.* **278,** 18817–18823
43. Romero, P., Obradovic, Z., Li, X., Garner, E. C., Brown, C. J., and Dunker, A. K. (2001) Sequence complexity of disordered protein. *Proteins* **42,** 38–48
44. Daher, W., Cailliau, K., Takeda, K., Pierrot, C., Khayath, N., Dissous, C., Capron, M., Yanagida, M., Browaeys, E., and Khalife, J. (2006) Characterization of *Schistosoma mansoni* Sds homologue, a leucine-rich repeat protein that interacts with protein phosphatase type 1 and interrupts a G_2/M cell-cycle checkpoint. *Biochem. J.* **395,** 433–441
45. Brady, M. J., and Saltiel, A. R. (2001) The role of protein phosphatase-1 in insulin action. *Recent Prog. Horm. Res.* **56,** 157–173
46. Ceulemans, H., and Bollen, M. (2004) Functional diversity of protein phosphatase-1, a cellular economizer and reset button. *Physiol. Rev.* **84,** 1–39
47. Newgard, C. B., Brady, M. J., O'Doherty, R. M., and Saltiel, A. R. (2000) Organizing glucose disposal. Emerging roles of the glycogen targeting subunits of protein phosphatase-1. *Diabetes* **49,** 1967–1977
48. Oliver, C. J., and Shenolikar, S. (1998) Physiologic importance of protein phosphatase inhibitors. *Front. Biosci.* **3,** D961–D972
49. Bennett, D. (2005) Transcriptional control by chromosome-associated protein phosphatase-1. *Biochem. Soc. Trans.* **33,** 1444–1446
50. Hirano, K., Erdödi, F., Patton, J. G., and Hartshorne, D. J. (1996) Interaction of protein phosphatase type 1 with a splicing factor. *FEBS Lett.* **389,** 191–194
51. Moorhead, G. B., Trinkle-Mulcahy, L., and Ulke-Lemée, A. (2007) Emerging roles of nuclear protein phosphatases. *Nat. Rev. Mol. Cell Biol.* **8,** 234–244
52. Novoyatleva, T., Heinrich, B., Tang, Y., Benderska, N., Butchbach, M. E., Lorson, C. L., Lorson, M. A., Ben-Dov, C., Fehlbaum, P., Bracco, L., Burghes, A. H., Bollen, M., and Stamm, S. (2008) Protein phosphatase 1 binds to the RNA recognition motif of several splicing factors and regulates alternative pre-mRNA processing. *Hum. Mol. Genet.* **17,** 52–70
53. Axton, J. M., Dombrádi, V., Cohen, P. T., and Glover, D. M. (1990) One of the protein phosphatase 1 isoenzymes in *Drosophila* is essential for mitosis. *Cell* **63,** 33–46
54. Baker, S. H., Frederick, D. L., Bloecher, A., and Tatchell, K. (1997) Alanine-scanning mutagenesis of protein phosphatase type 1 in the yeast *Saccharomyces cerevisiae*. *Genetics* **145,** 615–626
55. Chen, F., Archambault, V., Kar, A., Lio', P., D'Avino, P. P., Sinka, R., Lilley, K., Laue, E. D., Deak, P., Capalbo, L., and Glover, D. M. (2007) Multiple protein phosphatases are required for mitosis in *Drosophila*. *Curr. Biol.* **17,** 293–303
56. Ishii, K., Kumada, K., Toda, T., and Yanagida, M. (1996) Requirement for PP1 phosphatase and 20S cyclosome/APC for the onset of anaphase is lessened by the dosage increase of a novel gene *sds23*$^{+}$. *EMBO J.* **15,** 6629–6640
57. Thompson, L. J., Bollen, M., and Fields, A. P. (1997) Identification of protein phosphatase 1 as a mitotic lamin phosphatase. *J. Biol. Chem.* **272,** 29693–29697
58. Landsverk, H. B., Kirkhus, M., Bollen, M., Küntziger, T., and Collas, P. (2005) PNUTS enhances *in vitro* chromosome decondensation in a PP1-dependent manner. *Biochem. J.* **390,** 709–717
59. Lee, J. H., You, J., Dobrota, E., and Skalnik, D. G. (2010) Identification and characterization of a novel human PP1 phosphatase complex. *J. Biol. Chem.* **285,** 24466–24476
60. Blisnick, T., Vincensini, L., Fall, G., and Braun-Breton, C. (2006) Protein phosphatase 1, a *Plasmodium falciparum* essential enzyme, is exported to the host cell and implicated in the release of infectious merozoites. *Cell. Microbiol.* **8,** 591–601
61. Ward, G. E., Fujioka, H., Aikawa, M., and Miller, L. H. (1994) Staurosporine inhibits invasion of erythrocytes by malarial merozoites. *Exp. Parasitol.* **79,** 480–487
62. Ragusa, M. J., Dancheck, B., Critton, D. A., Nairn, A. C., Page, R., and Peti, W. (2010) Spinophilin directs protein phosphatase 1 specificity by blocking substrate-binding sites. *Nat. Struct. Mol. Biol.* **17,** 459–464
63. Dancheck, B., Nairn, A. C., and Peti, W. (2008) Detailed structural characterization of unbound protein phosphatase 1 inhibitors. *Biochemistry* **47,** 12346–12356
64. Huang, H. B., Chen, Y. C., Tsai, L. H., Wang, H., Lin, F. M., Horiuchi, A., Greengard, P., Nairn, A. C., Shiao, M. S., and Lin, T. H. (2000) Backbone ^{1}H, ^{15}N, and ^{13}C resonance assignments of inhibitor-2–a protein inhibitor of protein phosphatase-1. *J. Biomol. NMR* **17,** 359–360
65. Lin, T. H., Huang, Y. C., Chin, M. L., Chen, Y. C., Jeng, H. H., Lin, F. M., Shiao, M. S., Horiuchi, A., Greengard, P., Nairn, A. C., and Huang, H. B. (2004) ^{1}H, ^{15}N, and ^{13}C resonance assignments of DARPP-32 (dopamine and cAMP-regulated phosphoprotein, Mr. 32,000)–a protein inhibitor of protein phosphatase-1. *J. Biomol. NMR* **28,** 413–414
66. Huang, H. B., Chen, Y. C., Lee, T. T., Huang, Y. C., Liu, H. T., Liu, C. K., Tsay, H. J., and Lin, T. H. (2007) Structural and biochemical characterization of inhibitor-1α. *Proteins* **68,** 779–788
67. Dyson, H. J., and Wright, P. E. (2002) Coupling of folding and binding for unstructured proteins. *Curr. Opin. Struct. Biol.* **12,** 54–60
68. Terrak, M., Kerff, F., Langsetmo, K., Tao, T., and Dominguez, R. (2004) Structural basis of protein phosphatase 1 regulation. *Nature* **429,** 780–784
69. Hurley, T. D., Yang, J., Zhang, L., Goodwin, K. D., Zou, Q., Cortese, M., Dunker, A. K., and DePaoli-Roach, A. A. (2007) Structural basis for regulation of protein phosphatase 1 by inhibitor-2. *J. Biol. Chem.* **282,** 28874–28883
70. Marsh, J. A., Dancheck, B., Ragusa, M. J., Allaire, M., Forman-Kay, J. D., and Peti, W. (2010) Structural diversity in free and bound states of intrinsically disordered protein phosphatase 1 regulators. *Structure* **18,** 1094–1103
71. Pinheiro, A. S., Marsh, J. A., Forman-Kay, J. D., and Peti, W. (2011) Structural signature of the MYPT1-PP1 interaction. *J. Am. Chem. Soc.* **133,**

73–80
72. Egloff, M. P., Johnson, D. F., Moorhead, G., Cohen, P. T., Cohen, P., and Barford, D. (1997) Structural basis for the recognition of regulatory subunits by the catalytic subunit of protein phosphatase 1. *EMBO J.* **16,** 1876–1887
73. de Koning-Ward, T. F., and Gilson, P. R. (2009) Keeping it simple. An easy method for manipulating the expression levels of malaria proteins. *Trends Parasitol.* **25,** 4–7
74. Zhang, L., Qi, Z., Gao, Y., and Lee, E. Y. (2008) Identification of the interaction sites of Inhibitor-3 for protein phosphatase-1. *Biochem. Biophys. Res. Commun.* **377,** 710–713
75. Bharucha, J. P., Larson, J. R., Gao, L., Daves, L. K., and Tatchell, K. (2008) Ypi1, a positive regulator of nuclear protein phosphatase type 1 activity in *Saccharomyces cerevisiae*. *Mol. Biol. Cell* **19,** 1032–1045
76. De Wulf, P., Montani, F., and Visintin, R. (2009) Protein phosphatases take the mitotic stage. *Curr. Opin. Cell Biol.* **21,** 806–815
77. Wu, J. Q., Guo, J. Y., Tang, W., Yang, C. S., Freel, C. D., Chen, C., Nairn, A. C., and Kornbluth, S. (2009) PP1-mediated dephosphorylation of phosphoproteins at mitotic exit is controlled by inhibitor-1 and PP1 phosphorylation. *Nat. Cell Biol.* **11,** 644–651